

# Advancements in Passivating Contact and Structure Technology for Efficient, Cost-Effective, and Eco-Friendly Fabrication for c-Si Solar Cell Fabrication: A Comprehensive Review

Bhoora Ram<sup>1,a</sup>, Shrikant Verma<sup>2</sup>

<sup>1</sup>Research Scholar, Department of Physics, Poornima University, Jaipur, India.

<sup>2</sup>Associate Professor, Department of Physics, Poornima University, Jaipur, India

**ABSTRACT:** Global energy consumption has surged due to economic and population growth. Traditional fossil fuels are insufficient to meet daily energy needs and emit greenhouse gases, the main cause of global warming and climate change. Environmental concerns and increased energy demand are driving the adoption of alternative energy sources, particularly solar energy. Solar photovoltaic (PV) technology converts sunlight into electricity. The silicon heterojunction technology (SHJ) used in c-Si solar cells enabled a 26.7% efficiency by incorporating doped a-Si:H carrier selective contacts (CSCs) combined with an interdigitated back contact structure (IBC), which is less than the theoretical maximum limit of 29.43%. Solar cell performance is influenced by various energy losses like optical, recombination, electrical, and thermal. More parasitic absorption losses are caused by the doped a-Si:H, and doping with hazardous materials is costly and emits poisonous fumes. Mono-crystalline PV modules are also expensive. Transition metal oxides (TMOs) are abundant, non-toxic, and cost-effective have a broad range of band patterns, and have the virtue of carrier-selectivity, allowing only electrons or holes to flow through contact, which reduces recombination losses and parasitic absorption. TMOs can be used as an alternative to doped a-Si:H contacts. Advanced TMO passivating contacts, or heterocontacts, have emerged as a new industrially preferred technology that can be deposited by a simplified process at low temperatures with efficiencies exceeding 23.5% and a potential greater than 28.4%. This review discussed the recent research and innovations in passivating contact and advanced structure technology aimed at enhancing the performance and sustainability of c-Si solar cells. It focuses on technologies like silicon heterojunction, passivated emitter and rear cell (P.E.R.C.), interdigitated back contact (I.B.C.), heterojunction back contact (H.B.C.), and especially doping-free TMOs asymmetric heterocontact and their potential as cost-effective and eco-friendly alternatives. Passivating contact and structure technology has the potential to accelerate the transition towards clean, cost-effective, and sustainable energy production, providing a leveled cost of energy for society.

**Keywords:** crystalline silicon solar cell; passivating contact; solar cell structure technology; cost-effective; transition metal oxide (TMO); eco-friendly, carrier selective contact; titanium oxide ; molybdenum oxide.

## INTRODUCTION

Energy is a fundamental need for modern human life. Conventional energy sources like coal, oil, natural gas, and wood are non-renewable. Steam power and electrical power produced from fossil fuels like coal, gas, and oil have improved the quality of life but emit greenhouse gases that damage the environment (Liu Y et al., 2020). As fossil fuel resources deplete due to their continuous exploitation, this will end in the near future (Chander S. et al., 2022). Non-traditional energy sources such as hydropower, wind, tidal, geothermal, solar, and biomass are required. There is a need for alternative energy sources that are sustainable, renewable, and easy to maintain (Sharma S et al., 2015). Non-conventional energy sources like solar energy systems require low maintenance for decades and have no recurring costs once installed. Solar energy never runs out, is sustainable, environmentally clean, no charge, noise-free, & ubiquitous (Deshpande R.A. et al., 2021).

The sun emits energy through the nuclear fusion process, which creates a helium atom by combining four hydrogen atoms (Sharma S et al., 2015), and tremendous amounts of thermal energy are liberated. Radiant energy is environmentally clean, free of cost, noiseless, available abundantly, pollution-less, inexhaustible, ubiquitous, and free from other by-products (Chowdhury S et al., 2019). Crystalline silicon (c-Si) solar cells are the only non-traditional sources that can replace fossil fuels in an ecologically & economically viable manner (Sopian et al., 2017; Battaglia et al., 2016). Solar cells based on photovoltaic technology (PV) convert light energy into electrical energy (Ballif C. et al., 2022). Russell Ohl devised and patented the photovoltaic effect, which Edmond Becquerel observed; Charles Fritts created the first selenium solar cells; and Bell Labs produced the first silicon sun cell that could be used in practice in 1954 (Jingjing Liu et al., 2018). Mono-crystalline or polycrystalline silicon-based solar PV holds a market share of 95% due to its long-term stability over 25 years, reliability, and environmental friendliness (Yu Cao et al., 2018; Ballif C et al., 2022).

Solar energy can be utilized in two ways: photo-thermal and photovoltaic. Photo-thermal conversion uses solar radiation for applications like drying, water heating, and space heating, while photovoltaic conversion converts solar radiation into electricity (Deshpande R.A. et al., 2021). Alternative energy sources, like solar energy, are essential for a sustainable future. It requires lower workforce expenses than conventional energy production technology, but there is an initial expenditure on equipment such as solar cells, panels, and modules (Zeng Y et al., 2022). Under 1 sun illumination, a mono-junction silicon solar cell has a maximum efficiency limit of 29.43% (Shockley et al., 2004), but the maximum efficiency reached 26.7% at the cell level (Allen, T.G. et al., 2019) and 23.01% at the module level by using SHJ technology (Acharyya S et al., 2022; Masmitjà et al., 2022), have passivating contacts or carrier-selective contacts (CSCs) of doped a-Si:H and intrinsic amorphous silicon hydrogenated (i-a-Si:H) as passivation layers that reduced surface carrier recombination and improved charge carrier selectivity by using low contact resistance to pass one charge carrier and stop the others (Koswatta, P et al., 2015; 2022; Yan, D et al., 2022).

In SHJ solar cell doped p-type and n-type a-Si:H carrier selective contact's fabrication process is complicated by plasma enhanced chemical vapor deposition (PECVD) and doping of boron and phosphorus, which emit toxic and flammable gases and still remain energy losses by parasitic absorption and Auger recombination (Gerling L.G. et al., 2016; Scire D. et al., 2018). Well-passivating contacts reduce recombination losses; the indium tin oxide (ITO) coating and TMO contacts can increase carrier collection & decrease resistance losses (Zeng Y et al., 2022; Yu Cao et al., 2018). There are several high-efficiency c-Si solar cells that are made possible by advancements in the structure of c-Si solar cells; these include SHJ/HIT, P.E.R.C., I.B.C., & SHJ-IBC (H.B.C.) (Lin, H. et al., 2023). The doped a-Si:H layer still has energy losses from parasitic optical absorption and Auger recombination (Ibarra Michel et al., 2023), emits hazardous gases to damage the environment, and is also expensive (Chowdhury S et al., 2019). TMOs passivating contacts as an alternate to doped a-Si:H can reduce parasitic and Auger recombination losses (Mehmood H et al., 2020; Masmitjà et al., 2022), and TMOs are cost-effective, abundant, wideband structure, non-toxic, and eco-friendly (Yu Cao et al., 2018; Acharyya S et al., 2022).

Molybdenum trioxide and titanium dioxide function as hole-picking and electron-picking contacts, respectively, with the SiO<sub>2</sub> passivation layer, achieving an efficiency of more than 23.5% by a simplified process at low temperatures less than 200°C with SHJ structure technology (Scire, D et al., 2018; Dréon J et al., 2020; Tyagi A et al., 2021; Chee, K.W. et al., 2022; Yan D et al., 2022), efficiency of the n-Si/SiO<sub>x</sub>/TiO<sub>x</sub>/Al contact is 24.1% (V. Titova et al., 2021), 24.83% was numerically demonstrated (Mehmood H et al., 2020), and it has a potential greater than 28.4% (Yu Cao et al., 2018; Ibarra Michel et al., 2023).

The scheme's TMO passivating contact evolution triggered the (c-Si) solar cell technical revolution (Sanyal Set et al., 2019; Wang Y et al., 2022). Research focuses on increasing efficiency and limiting production costs using advanced passivating contact and structure technology for the performance improvement of solar power devices. This review analyses innovative solar cell manufacturing techniques from an economic perspective and evaluates passivation schemes using materials like TMOs. Key factors affecting efficiency include structure, process optimization, and cost-reduction strategies (Chang N.L. et al., 2023). The cost of manufacturing will go down as solar cells' efficiency rises, enabling our society to access the leveled cost of electricity (LCOE) (García-Hernansanz et al., 2023; Acharyya S et al., 2022).

### **Solar cell working/operating principle**

c-Si operating circuit as shown in figure.1, the functioning of solar cells involves three steps: the generation of electron-hole pairs by light absorption, the separation of charge carriers, and the collection of hole-electrons at the appropriate contacts. A solar cell is a semiconductor junction diode; the n-section is narrower than the p-section to facilitate fast electron passage across the circuit and current generation before the electrons recombine with the holes (Ezzi A et al., 2022). When photons from the solar radiation incident on a solar cell are absorbed, electrons in the valence band are excited and move to the conduction band by creating a significant amount of holes in the valence band. Both the electrons and holes are generated in the depletion layer of the junction diode.

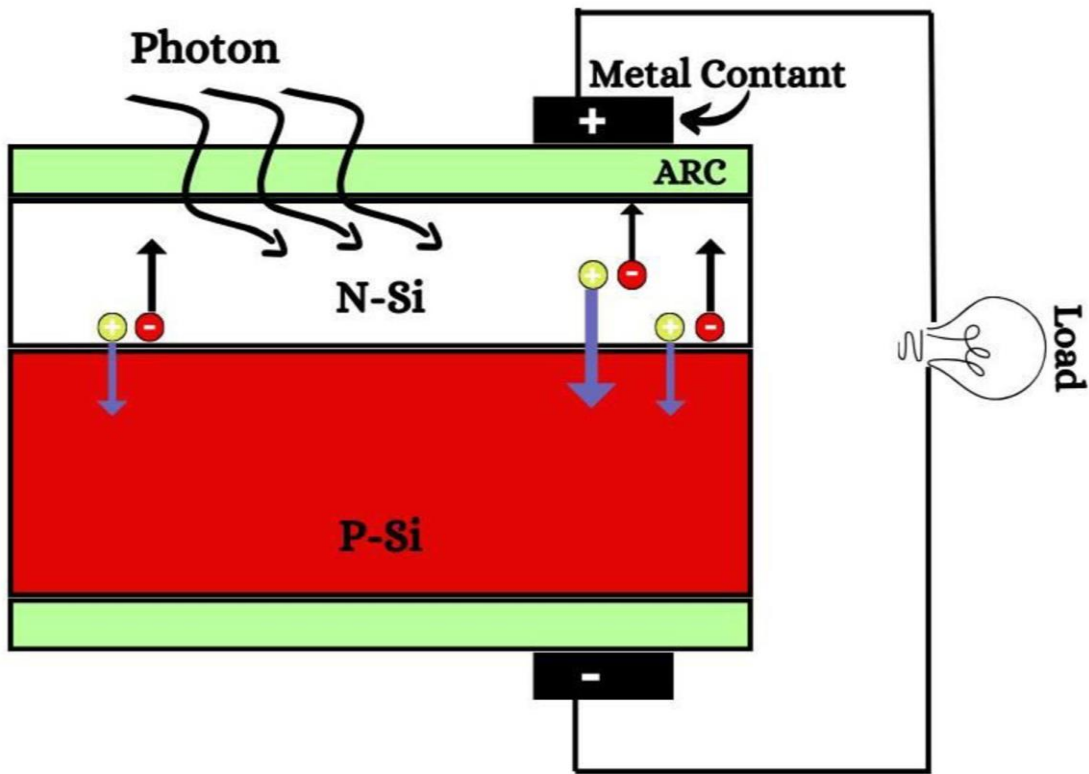


Fig.1 Solar cells working/ operating principle

Excess energy in a semiconductor is released as heat, causing total electron and hole concentrations to diverge from their thermal equilibrium in the absence of light (Acharyya S et al., 2022). When electron-hole couples in the space charge area and holes in the p-section are separated by the inherent electric field, a photogenerated electric field is produced. The PV effect, a photoelectromotive force that partially counteracts the inherent electric field, causes the n-type section to become negatively charged & the p-section to become positively charged (Sui et al., 2021). The solar cell needs to be connected to an external circuit by means of contacts in order for electric current to flow through it. In short circuits, the current peaks at zero voltage; however, external shunts and internal recombination losses might affect this. To reduce surface reflection and increase light transmission, an anti-reflective substance is applied to the n-layer (Jingjing Liu et al., 2018).

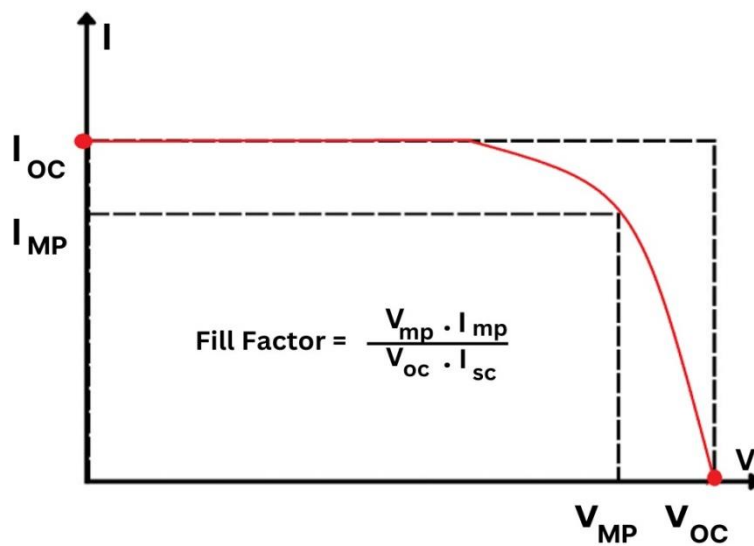


Fig. 2 I-V characteristics curve of solar cells.

When no current flows through the contacts, the maximum potential across the contacts is called open-circuit-voltage ( $V_{oc}$ ), and the maximum current that may flow in the outer circuit in the zero resistance is referred as short circuit current ( $I_{sc}$ ). Current density ( $J_{sc}$ ) is the amount of  $I_{sc}$  flow per unit cross-sectional area. I-V characteristics curve used to determine these solar cell properties as shown in figure 2.

Equivalent solar cell circuit described in Figure 3

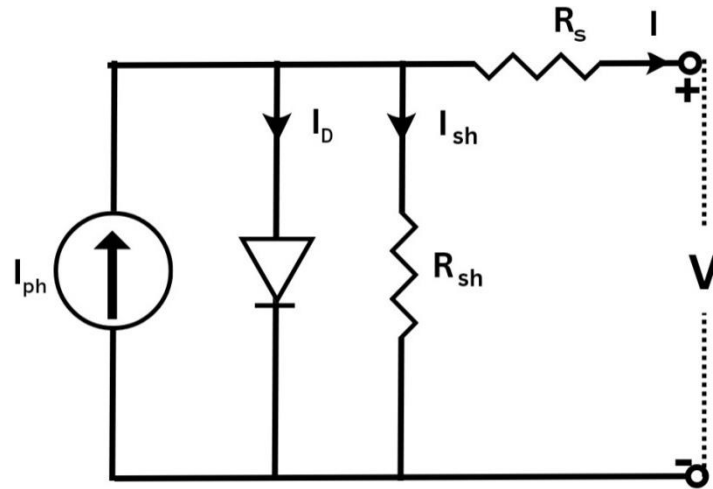


Fig. 3 Solar cells equivalent circuit

The total current flow in equivalent circuit is given by

$$I = I_{ph} - I_d - I_{sh}$$

Where  $I_d$  is diode current,  $I_{ph}$  is a photocurrent,  $I_{sh}$  is shunt current (Kodati et al., 2020, Al-Ezzi et al., 2022).

Diode current is given by formula as below

$$I_d = I_0 [e^{V/\alpha kT} - 1]$$

Where  $I_0$  is dark or maximum reverse saturation current,  $\alpha$  is ideality factor

Shunt current is given by

$$I_{sh} = \frac{V + IR_s}{R_{sh}}$$

Where  $R_s$  is series resistance.

The fill factor is the maximum power density divided by the product of  $J_{sc}$  and  $V_{oc}$ .

$$FF = \frac{I_{max} \cdot V_{max}}{I_{sc} \cdot V_{oc}}$$

The ratio of power gained from cells to power delivered to cells is known as power conversion efficiency (PCE)

$$PCE (\eta) = \frac{P_{out}}{P_{in}} = \frac{I_{max} V_{max}}{P_{in}} \times 100\%$$

Where 'Pin' is the incident power density, 1000 W/m<sup>2</sup>

$$PCE (\eta) = \frac{I_{sc} \cdot V_{oc} \cdot FF}{P_{in}} \times 100\%$$

PV cells, when connected in series and parallel, can produce specific power outputs, with six cells generating the same current and ideal 3 V. (Al-Ezzi et al., 2022).

### Solar cell's generations & its types

Three generations of solar cells are distinguished: wafer technology (first generation), thin-technology (second generation), and emerging technology (third generation) as shown in figure 4.

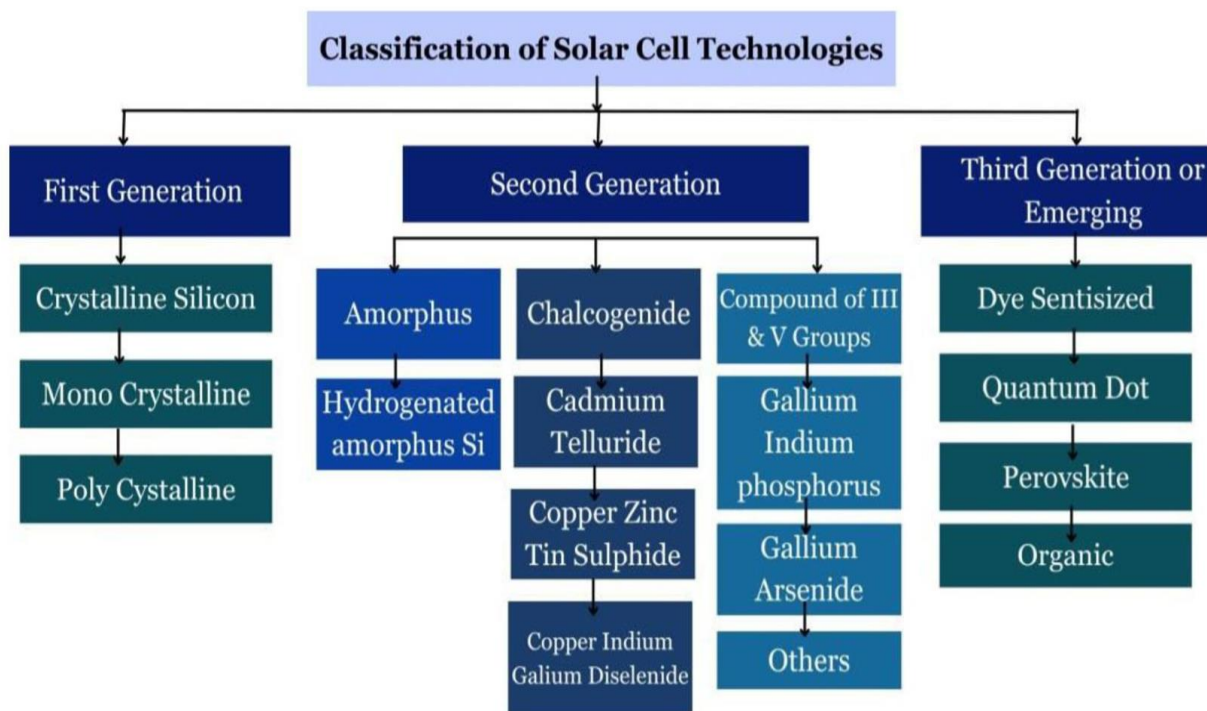


Fig. 4 Classification of solar cells technologies

Wafer technology (first generation) solar cells are found in mono-crystalline and poly-crystalline wafers, while thin-film technology (second generation) includes amorphous silicon, CdTe, and C.I.G.S., emerging technologies (third generation) include D.S.S.C., quantum dots, organics, perovskites, tandem solar cells, etc. (Badawy, 2015). The solar cell technologies are categorized as follows:

**Wafer technology (first generation)**

In this generation, silicon wafers are used for fabrication, the oldest and most popular technology. Its sub-groups are mono-crystalline and poly-crystalline silicon solar cells (Acharyya S et al., 2022). Mono or single-crystalline solar cells are produced using the Czochralski process, a precise and expensive re-crystallization process with efficiency ranging from 17% to 24%, requiring precise processing from large ingots. Polycrystalline solar cells are composed of multiple crystals in a single cell, created by chilling a graphite mould that has silicon molten inside of it. They are the most popular solar cells and are less efficient than mono-crystalline silicon ones, although they are slightly less expensive to manufacture, accounting for 12.1% to 14% of the total (Sharma S et al., 2015).

Table 1. Mono- crystalline & poly-crystalline solar cells and their efficiency and properties.

Sub group of wafer technology	$\eta$ %	Properties
Single crystalline solar cells	17 to 24	High efficient, expensive, and complex manufacturing process than poly-crystalline solar cells.
Poly-crystalline solar cells	12.1 to 14	Cheaper but less efficient than mono-crystalline solar cells.

**Thin-film technology (second generation)**

Thin-film solar cells are made of amorphous silicon, CdTe, and C.I.G.S.; they are less expensive and thinner than silicon wafer cells. Thin-film solar cells degrade in the environment, achieving an efficiency of 5–7% (Ezzi A et al., 2022). Thin film solar cells are as follows:

**Amorphous silicon thin film solar cell**

Amorphous silicon thin film solar cells, fabricated by doping silicon material on a substrate or glass plate, are inexpensive and widely available due to their non-crystalline structure and lack of fixed atom arrangements. However, their efficiency is

poor and unstable, falling short of that of commercial PV modules. Amorphous silicon solar cells, with a doped silicon material on the back side, are ideal for varying climatic conditions and can operate at high temperatures, enhancing light absorption (Ezzi A et al., 2022; Kodati et al., 2020).

#### Cadmium Telluride (CdTe) solar cell

Cadmium telluride (CdTe) is a cost-effective photovoltaic material with a 1.5 eV band gap, excellent stability and absorption of light, the direct band gap semiconductor characteristics of which make it perfect for thin-film solar cells (Ezzi A et al., 2022). Cadmium sulphide layers are sandwiched to provide p-n junction diodes in CdTe solar cells, synthesized from polycrystalline materials and coated with multiple layers on the substrate, making them flexible and available on polymer substrates. Cadmium telluride, a hazardous heavy metal, causes severe environmental damage (Sharma S et al., 2015).

#### Copper- Indium- Gallium- Di-selenide (C.I.G.S.)

C.I.G.S. is made up of copper, indium gallium, and selenium and has a small band gap ranging from 1 to 1.7 eV. It is deposited through thermal evaporation, an electron evaporator, or sputtering. With a five-layer structure with substrates like glass plates, polymers, steel, and aluminium and a higher efficiency of 10% to 12%, CIGS is a popular thin film technology for solar cells (Deshpande R.A. et al., 2021; Kodati et al., 2020).

**Table 2. Second generation solar cells and their efficiency and properties (Al-Ezzi et al., 2022)**

Name of Thin film solar cell	Efficiency	Properties
a-Si	05-12 %	Light in weight, cheaper, absorbs more energy than c-Si but less efficiency
Cadmium telluride	15-16 %	Good performance at high temperature, cheaper but toxic
CIGS	20.0 %	Good performance at high temperature, cheaper but toxic, low stability and have complex structure.
Gallium arsenide	28.7%	Ga expensive, low abundance and As is highly toxic.

#### Emerging technology (third generation).

Emerging technology solar cells include QD, polymer & organic, dye-sensitized, concentrated, perovskites, kesterite, and tandem solar cells. These cells are introduced to reduce production costs and increase power conversion efficiency (PCE) as follows:

#### Dye Sensitized (D.S.S.C.) Solar Cell

The D.S.S.C. is a low-cost, flexible solar cell technology that operates similarly to photosynthesis. A conductive support system, a semiconductor sheet, dye, electrolyte, and counter electrode are its five constituent parts. Efficiency can be increased by fine-tuning components. DSSCs are designed considering optoelectronic properties like absorption coefficient, band alignment, dye morphology, and assembly mode on the TiO<sub>2</sub> photo-anode, and conversion efficiencies of over 11% and 15% have been achieved in laboratory studies. However, challenges like dye degradation and stability issues persist (Sharma S et al., 2015).

#### Kesterite solar cells

Kesterite solar cells, made from copper-zinc-tin-sulphide and copper-zinc-tin-selenide, have similar optical and electronic properties to CdTe and CIGS but lack toxic elements Cd and In. They have an efficiency around 8% with CZTS cells and around 10% with CZTSe cells, but face limitations like dominant interface recombination & less minority carrier lifetime (Deshpande R.A. et al., 2021; Sharma S et al., 2015).

#### Polymer and organic solar cells

Flexible solar cells made of thin layers coated on a polymer sheet are known as polymer solar cells. They function as a combination of a polymer and fullerene and can be made from various materials for sunlight absorption. Organic solar cells, thin film cells using organic semiconductors, offer advantages like affordability, flexibility, and light weight but have low efficiency. Organic solar cell belongs to the excitonic solar cells category. When light is incident on a cell, it produces bound electron-hole pairs, with absorbent materials like poly(3-hexylthiophene) (P3HT), phthalocyanine, and 6,6'-phenyl-C<sub>61</sub>-butyric acid methyl ester (PCBM). When a photon is absorbed in an organic semiconductor, it excites one electron to valence band and leaves behind a hole in the conduction band. (Acharyya S et al., 2022). These holes and electrons remain bound due to coulombic forces. If the junction is composed of two distinct organic materials, efficient charge separation of exciton and free carrier production may take place. The bulk hetero-junction increases the donor-acceptor interface area, allowing each to be thinner around the junction. The bi-continuous phase separated network at the donor-acceptor interface separates excitons generated in donor material due to photon absorption. In commercial organic solar cells, a combination of P3HT (Donor) and PCBM (acceptor) is used to achieve an efficiency of about 5%. Metals like Al, Ag, and Au are also used for the back electrode (Kodati et al., 2020).

#### Perovskite solar cells

It is anticipated that perovskites, a kind of chemical with the formula  $ABX_3$ , will be important for electric car batteries due to their efficiency of up to 31%.  $MgSiO_3$ , abundant in magnesium silicate, offers low recombination losses, low material cost, and a longer charge carrier diffusion length.  $CH_3NH_3PbI_3$  used for high-efficiency perovskite solar cells. However, perovskite degrades over time, with a best lifetime of 10,000 hours but low stability, much shorter than the 25 years expected from commercialized PV technologies (Sharma S et al., 2015; Acharyya S et al., 2022).

### Quantum - dot solar cells

Quantum dots (QD) solar devices, introduced by Burnham and Duggan in 1989, are a technology with a variable band gap that can be adjusted by changing the size of artificial atoms, with an efficiency of 18.1%. QDs are composed of semiconductors from transition metal groups, such as porous Si or  $TiO_2$ . Advancements in nanotechnology have led to their use as an alternative to bulk materials like Si, CdTe, or CIGS. Colloidal CdX is the most investigated QD, known for its excellent optical and electrochemical properties. QDs are ideal absorber materials in third-generation photovoltaic cells, with a maximum efficiency of 16% using hot photo-generated carriers (Kodati et al., 2020).

### Tandem solar cells

Tandem solar cells feature various p-n junctions made of semiconductor material that are linked one after the other from the top to bottom. The p-n junction's varied band gap allows it to absorb different wavelengths of sunlight and create more electric current, which is short circuit current, increasing its efficiency. It offers a high power conversion efficiency of up to 36% and is reasonably priced. The top-to-bottom p-n junction has a decreasing band gap, therefore the higher cell generates more photocurrent than the lower cell. Tandem cells have an efficiency greater than 36%, which exceeds the Shockley-Quisser limit. The combination of groups III and IV, such as Ga-As and In-Ph, can enhance efficiency but is costly.

**Table 3. Third generation solar cell , their efficiency and properties**

Name of Solar cells	Efficiency	Properties
D.S.S.C	05 to 20 %	Semi - flexible, Low cost but low stability .
Organic/Polymer solar cells	09 to 11 %	Light, flexible, less life time, low efficiency.
Perovskite solar cells	21.0 %	Cheaper, good thermal stability but toxic
Quantum-dots solar cells	11to 17 %	Have ability to tune bandgap but less efficient.
Multi-junction solar cells	36.0 %	Highly efficient but more expensive.

### Surface Passivation

Solar cell efficiency may be increased by surface passivation and passivated connections. Surface passivation involves inserting a thin layer of  $SiO_2/Al_2O_3/a-Si:H$  between the silicon surface and the passivating contact, which prevents electrons and holes from recombining before they reach their respective contacts ( Bullock J et al., 2016). Passivating interlayers like silicon oxide and  $i-a-Si:H$ ,  $SiNx$ , are used in solar cells to reduce surface recombination and interface traps. Chemical passivation prevents electron and hole recombination, while charge carriers are repelled away from the interface by an electric field created by field-effect passivation (Geling LG et al., 2017; Masmitjà et al., 2022). The passivation layer lowers surface dangling bonds, and recombination loss is decreased when metal-Si contact areas are smaller. Charge recombination losses produced by defect states at metal-absorber interfaces are a significant contributor to efficiency improvement. Resolving this problem by lowering the metal-absorber contact area utilizing partial rear contact (P.R.C.) and P.E.R.C. Contacts constructed of metal oxide with substantial doping and blocking one kind of carrier on the defective interfacing and the substances intrinsic amorphous ( $i-a-Si:H$ ),  $SiO_2$ , and  $Al_2O_3$  are employed as rear passivation and full area passivation in various solar cell technologies to minimize recombination loss and contact resistance for improvement of efficiency (Zhao, Y et al., 2023).

### Radiative, non-radiative and defect assisted recombination losses

Charge carriers in the meta-stable state achieve equilibrium by electron and hole recombination via radiative, non-radiative (or Auger), and defect-assisted recombination (or Shockley-Read-Hall). When charge carriers recombine directly with the ejection of photons, this is called radiative recombination. When electrons and holes recombine in Auger recombination, energy is given to the third particle, which collide the phonon of the lattice and loses its energy (Acharyya S et al., 2022). Excessive doping in c-Si causes non-radiative recombination losses. Defects and flaws in silicon wafers cause Shockley-Read-Hall (SRH) recombination as shown in figure.5 The recombination kinetics of photo-generated excess carriers are used to compute the minority-carrier recombination life-time ( $\tau_{eff}$ ), which is the mean time that a minority carrier may stay excited after electron-hole creation before recombining, and it is affected by the kind of recombination events in silicon determined by the Quasi-steady-state photo-conductance (QSSPC) method (Zhao, Y et al., 2023; Richter A et al., 2021). The QSSPC approach detects a temporal photo-conductance signal produced by the sample, allowing the estimation of excess carrier

density and distinguishing itself from other approaches by producing absolute measurements of surplus carriers throughout a broad range of light intensity variations (Flathmann C et al., 2023).

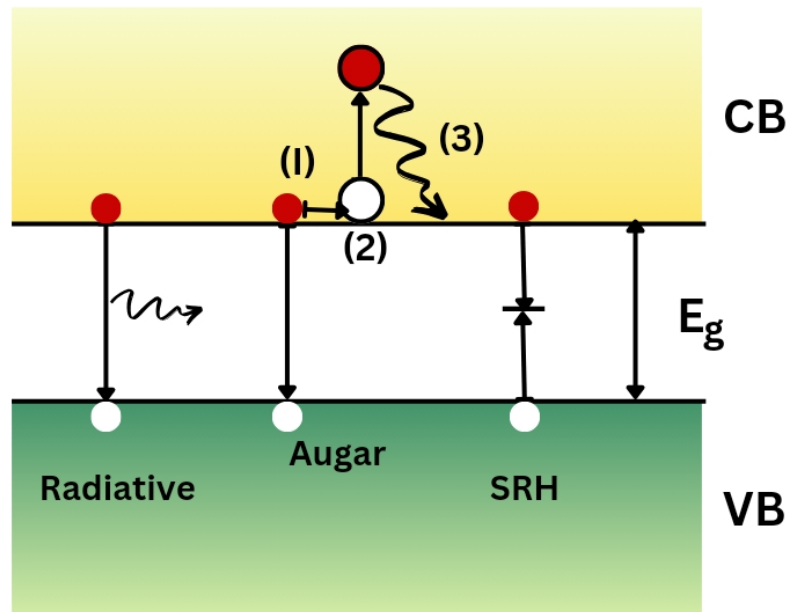


Fig. 5 Radiative, non-radiative and defect assisted recombination losses

#### Recombination current density ( $J_{oc}$ ) & Minority carrier lifetime ( $\tau_{eff}$ )

Recombination at the interface between metal oxide and silicon can negatively impact solar cell performance by reducing the available electrons and holes for collection, thereby decreasing efficiency. High-efficiency solar cells must have fewer recombination losses, which means a lower recombination current density. This will be accomplished by appropriate passivation. If the surface recombination velocity (SRV) is high, a considerable proportion of carriers recombine before they reach the contact. As a result, short-circuit current is decreased, and cell efficiency decreases. To prevent recombination, a thin layer of insulator is applied on the silicon substrate. When SRV is less than 10 cm/s, the recombination rate slows, increasing the efficiency of solar cells (Masmitjà et al., 2022).

Recombination current density ( $J_{oc}$ ) is determined by measuring charge density and recombination rate at the open circuit (Acharyya S. et al., 2022; Melskens J. et al., 2018). Minority carrier lifetime is the average time taken for recombination by an excess minority carrier; the lifetime can be as high as 1 millisecond in silicon (Acharyya S et al., 2022; Liu Y et al., 2020). The lifetime depends on the number of defects and the magnitude of radiative or Auger recombination. Minority carrier lifetime and diffusion length are two recombination rate-related characteristics. Minority carriers have a long lifespan and can readily reach their respective contacts, which increases solar cell current and efficiency (Nayak M et al., 2019).

#### Contact resistivity ( $\rho_c$ )

A contact refers to the interface between a metal and a silicon surface, affecting charge carrier flow through passivated contacts. When the contact resistance between the Si substrate and the metal contact is low, charge carriers may readily pass the junction, increasing the electric current. Charge carrier collection and extraction take place at metal-silicon contact and are impacted by  $T_o$  to increase solar cell efficiency, contact resistance should be reduced. The Cox and Strack technique determines contact resistivity ( $\rho_c$ ).

Contact resistance between Molybdenum oxide and silicon surfaces is tested by placing an Al back surface contact and a circular array with varying diameters on the front surface. (Bullock J. et al., 2018; Geling LG et al., 2017; Vijayan ; R.A. et al., 2019).

#### Carrier-selective contacts (CSCs)

In SHJ solar cells, doped a-Si:H and transition metal oxides (TMOs) like  $TiO_2$  and  $MoO_3$  work as carrier-selective or passivated contacts. Contacts and interfaces perform both carrier-selectivity and passivation, enabling one type of charge carrier to pass while damming up the other. It's called passivating contacts. Passivating contact reduces the conductivity of one carrier, preventing it from travelling across interfaces, while boosting the conductivity of the other carrier, allowing it to flow freely away from the interface. Passivated contacts regulate the mobility of charge carriers owing to conductivity asymmetry. Selectivity is obtained by regulating the charge carrier concentration on the surface and generating asymmetric conductivity by passivating contact, which is made feasible by negative fixed charges and metal oxide's high work function. Passivated contacts reduce contact resistance and recombination current density, which improves solar cell performance. Fermi level pinning is reduced by sandwiching a  $SiO_2$  layer between the metal oxide and Si surfaces (Geling LG et al., 2017).



TiO<sub>2</sub> is an electron-selective contact due to its smaller conduction band offset and larger valence band offset with silicon, while MoO<sub>3</sub> and NiO are hole-selective contacts due to their wide conduction band offset and smaller valence band offset. When the TMO's conduction band energy is higher than the Si layer's valence band energy, surplus holes undergo band-to-band tunnelling.

Charge carriers flow asymmetrically within the solar cell in the direction of the contact areas due to the charge-carrier selectivity at the terminals. The open circuit voltage (V<sub>oc</sub>) significantly indicates the suppression of non-collected charge carriers towards the opposite polarity contact (Mallem et al., 2019; Acharyya S et al., 2022).

#### Structure/Architecture technology of c-Si solar cell.

c-Si solar cell structure technology produces various high-efficiency solar cells, including passivated-emitter-rear-cells (P.E.R.C.), interdigitated-back-contact-cells (I.B.C.), silicon heterojunction technology (SHJ/HIT), and a combination of SHJ and IBC called hetero-back contact (H.B.C.). The silicon solar cell has evolved from a normal back surface field to P.E.R.C., HIT/SHJ, TOPCon, & IBC-SHJ structures, the primary advancement being the implementation of entire area, partial, and back surface passivation, and I.B.C., where there are no metal contacts or shading losses on the front surface. Materials with favorable tunneling characteristics, such as SiO<sub>2</sub>/SiN/Al<sub>2</sub>O<sub>3</sub>, can be used for full-area passivation (Liu Y et al., 2020). The highest cell efficiencies were reported for P.E.R.C. at 24.06%, for H.I.T. at 25.6%, for TOPCon at 25.7%, for DASH with SHJ exceeding 23.5%, and for I.B.C. with heterojunction back contact (HBC) at 26.7% (Liu Y et al., 2020).

#### The Passivated Emitter and Rear Cell (PERC) structure

The passivated emitter and rear cell (PERC) structure, as shown in Figure 6, first developed in 1983, improves light capture near the rear surface of crystallinity silicon solar cells. LONGI Solar has developed a new technology using a back surface field (B.S.F.) cell architecture with a Al deposition on the back side and a dielectric passivation layer, Al<sub>2</sub>O<sub>3</sub>/SiN<sub>x</sub>, to reduce optical and electrical losses. The PERC structure achieved a record efficiency of 24.02% in 2019. Further optimisation on the front end, like novel metallization ideas and enhanced junction characteristics, could potentially boost cell performance. Future research should focus on developing doping of the emitter layer and local BSF processes for high-quality fabrication (Jingjing Liu et al., 2018; Acharyya S et al., 2022).

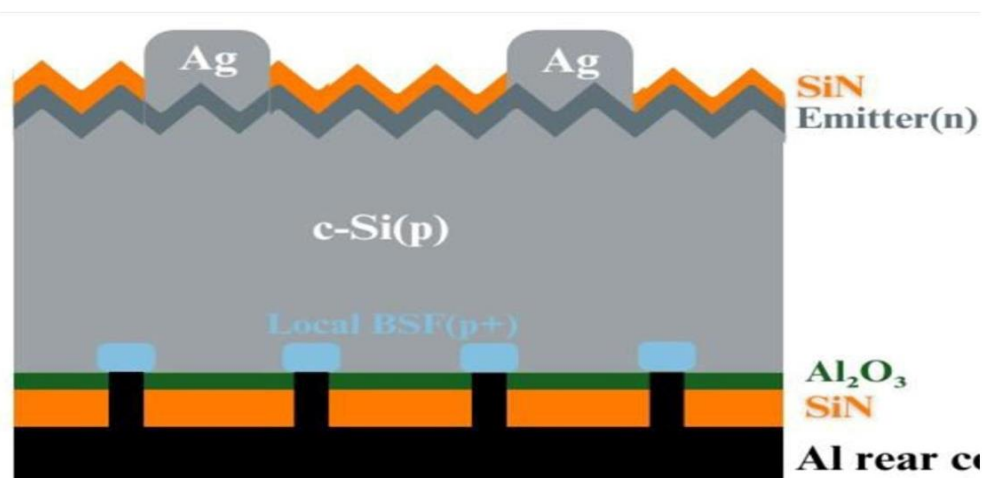
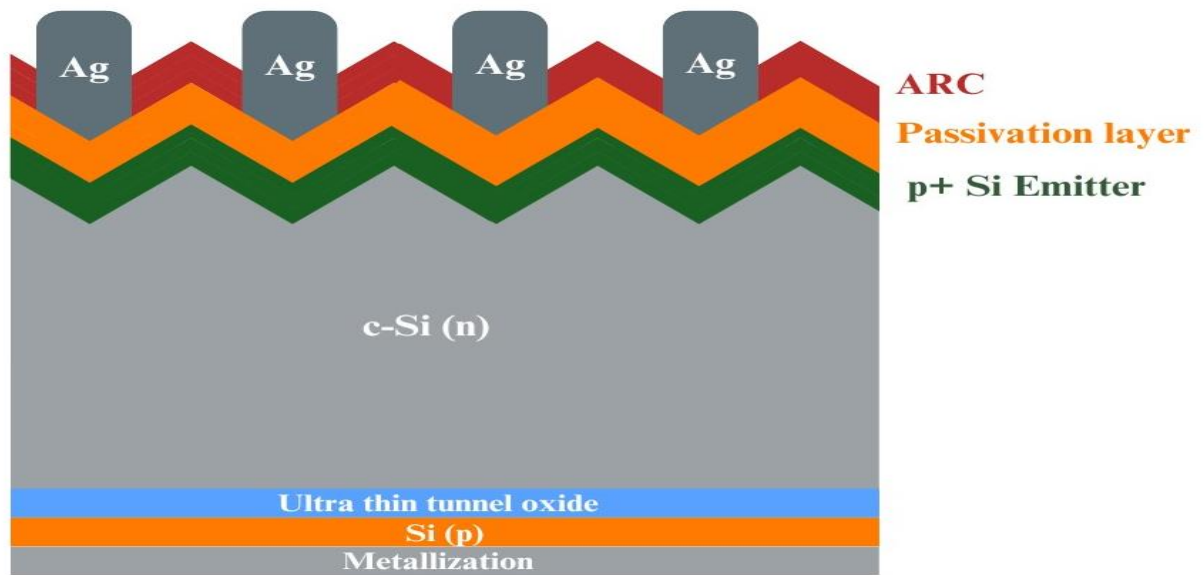


Fig. 6 P.E.R.C.solar cell

#### Tunnel oxide passivating contact (TOPCon) solar cell structure

The TOPCon cell structure as shown in Figure 7. TOPCon solar cell was created using an ultrathin SiO<sub>2</sub>/SiN layer, a pentavalent phosphorus (P) doping silicon layer, and a poly-silicon film to create the tunnel oxide passivating contact cell structure. Physical vapour deposition is used to deposit Ag on the back contact. The TOPCon design achieved a 23.0% conversion efficiency, high temperature stability, and simplified fabrication (Yang X et al., 2016; Wong T.K. et al., 2020). TOPCon technology comprises metal contacts on both sides and full-area passivated rear contacts, eliminating patterns from the back side. As a result, the width of the intervening SiO<sub>2</sub> passivation layer permits charge carriers to pass through it. The TOPCon backside structure, coated with highly doped silicon, achieves a record efficiency of 25.7%. (Liu Y. et al., 2020).



**Fig. 7 Tunnel oxide passivated contact solar cell structure**

**Poly-crystalline Si on oxide (POLO) solar cells structure**

The poly-crystalline Si on oxide (POLO) solar cell structure is shown in Figure 8.

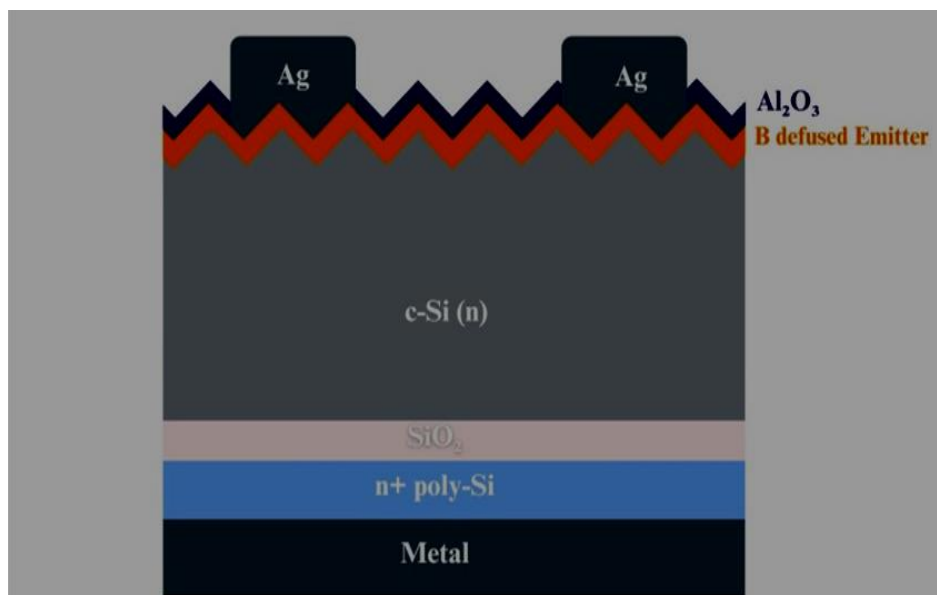


**Fig. 8 POLO solar cell structure**

Poly-silicon passivating contacts (poly-Si) have been used in silicon solar cells since the 1980s, offering a high fill factor and efficiency of more than 25% for large- areas (Liu Y et al., 2020). The PV industry is drawn to these connections because they can withstand the high temperatures required for screen printing. A highly doped poly-Si layer and an ultra-thin silicon oxide (SiO<sub>2</sub>) make up the poly-Si structure (Zhao, Y. et al., 2023). The interfacial oxide is formed, poly-crystalline silicon layers are deposited, and doping is added during the process. Usually, the poly-Si layer is placed on the back surface to reduce parasitic absorption (Yu Cao et al., 2018). The performance of both-sides-contacted solar cells can be categorized into front and rear junctions, with the rear junction configuration achieving the highest efficiency at 26.0%, but the use of poly-Si in industrial cells results in significant front surface recombination (Wong T.K. et al., 2020; Ibarra Michel et al., 2023).

**I.B.C. structure solar cell**

I.B.C. structure solar cell is shown in Figure 9. For effective light trapping on silicon wafers, front surface texturing with random pyramids is used throughout the fabrication process, while The back surface has been polished. Both the emitter and rare-surface field doping layers are located in an interdigitated structure on the back side of the cell, eliminating optical shading losses and increasing short-circuit current density and absorption capacity (Yoshikawa K et al., 2017 ;Liu Y et al., 2020). IBC solar cells are cost-effective for solar energy applications, but they can increase costs and have issues with

alignment and repeatability (Wang Z et al., 2019; Ibarra Michel et al., 2023). Laser doping techniques offer homogeneous doping concentration, controllability of depth, ability to build patterns, and protection of certain doping areas. Ion implantation is widely used in the semiconductor industry to precisely control doping concentration, while laser doping offers benefits including the capacity to easily manage the doping area's design without lithography and the doping depth and concentration.

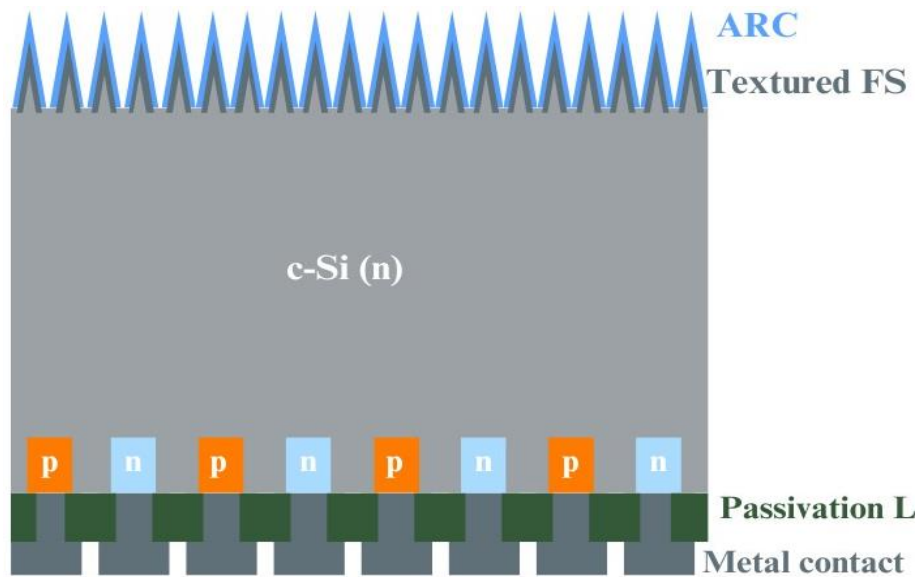


Fig.9 I.B.C. cell structure

The high efficiency, coplanar connections for solar panels, and almost negligible reflection of I.B.C. solar cells make them appealing. However, a significant obstacle to large-scale manufacture continues to be their high cost as a result of their intricate fabrication process (Jingjing Liu et al., 2018; Sui et al., 2021; Wong T.K. et al., 2020).

#### Silicon heterojunction SHJ/HIT structure solar cells

The silicon heterojunction SHJ/HIT structure solar cells is shown in Figure 10. In SHJ technology, utilizing pure a-Si:H layers in between doped contacts and silicon wafers has the ability to minimize recombination losses. The hydrogenation of crystalline silicon surface states causes passivation, resulting in a high  $V_{oc}$ . However, unpassivated dangling bonds near the surface can produce defects, which can be resolved by chemical passivation, which involves passivating the dangling bonds with hydrogen. This strategy has the ability to improve  $V_{oc}$  and the efficiency ( $\eta$ ) of heterojunction technology (Chang, N.L. et al., 2023). Photovoltaic cell technology employing a heterojunction between semiconductors with varying band gaps is known as silicon heterojunction solar cells (SHJ) or HIT.

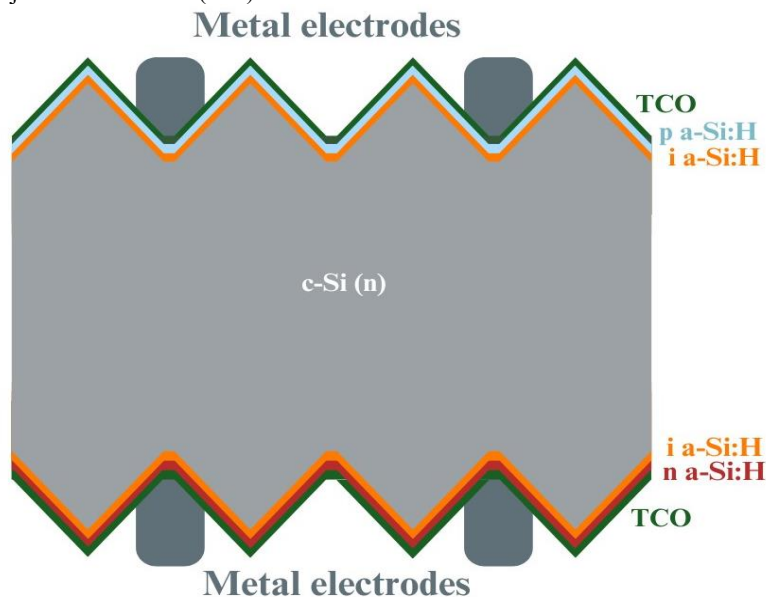


Fig.10 silicon heterojunction SHJ/HIT structure solar cells

Initially called HIT, it is now simply SHJ. The SHJ/HIT solar cell was first designed by Sanyo Co. Ltd. in 1991 and consists of n-type and p-type doped hydrogenated amorphous silicon carrier selective contacts on crystalline silicon substrates, an intrinsic amorphous silicon hydrogenated surface passivation layer on both sides, a transparent conductive oxide layer of indium tin oxide on a p-type a-Si:H contact, and a metal electrode (Richter A et al., 2021). These solar cells were the first to use crystalline silicon with a larger bandgap "passivating contact" for high efficiency using doped and intrinsic hydrogenated amorphous silicon layers for carrier selectivity and excellent chemical passivation carrier selectivity (Zhao, Y et al., 2023). Surface texturing and cleaning are the first steps in the fabrication process. The silicon wafer is then passivated on both sides with a thin coating of inherently hydrogenated amorphous silicon. These heterocontacts inhibit charge carrier recombination and parasitic absorption, increasing efficiency by up to 25.1%. Kaneka Company obtained the best efficiency of c-Si solar cells (26.7%) using SHJ, which is based on simpler processes and higher-level production with the IBC framework (Wong T.K. et al., 2020).

#### Hetero back contact (H.B.C.) structure solar cells

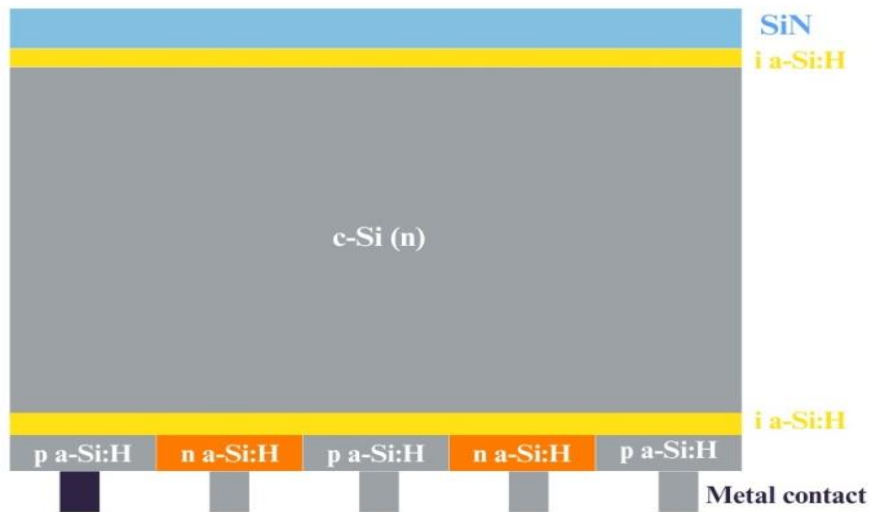


Fig.11 Heterojunction Back Contact (HBC) structure solar cells

The H.B.C. structure of solar cells is seen in Figure 11. Kaneka (now Panasonic) developed the SHJ-IBC structure, which decreases the shielding effect and achieves an efficiency of up to 26.7%. It is also known as revolutionary technology due to its high passivation, which increases both the short-circuit current density and the open-circuit voltage. It has two stacking layers: the front surface is textured with a passivation layer, and the back is a silicon nanolayer with a grid electrode. HBC structure aids in the inhibition of recombination, light reflection, and series resistance (Bivor et al., 2017)

Table 4: cell structure -based efficiency

Cell structure	Wafer type	Voc (mV)	Jsc (mA · cm <sup>-2</sup> )	FF (%)	Effic. (%)
P.E.R.C.	n- type Floate zone	-	-	-	23.3
TopCon	n- type Floate zone	725.1	42.60	83.2	25.6
I.B.C.	n- type Floate zone	737.1	41.34	82.6	25.1
S.H.J.	n- type Floate zone	738.0	40.81	83.4	25.2
H.B.C	n- type Floate zone	742.5	42.51	42.4	26.7

#### TMOs contact based SHJ solar cells technology

Titanium oxide and molybdenum trioxide, known as transition metal oxides (TMOs), are used as carrier selective contacts. TMOs with passivated contacts can prevent recombination while also allowing charge carrier extraction. TMOs are plentiful, inexpensive, and readily deposited as a thin layer utilised as passivated contacts, creating an extraction barrier and demonstrating electrical conductivity. A new TMO thin layer and flexible cell technology has the potential for unique cell design and manufacture of solar cells with long-term sustainability and performance (Geling LG et al., 2017; Greiner MT et al., 2012).

#### Basic of transition metal oxides

TMOs exhibit a variety of electrical, catalytic, structural, optical, and nontoxic characteristics. TMOs feature a wide band gap, a diverse variety of work functions, high transparency, low temperature deposition using simpler procedures, and are less expensive. TMOs' work functions are dependent on partially filling 2p-orbitals of O2 and partially filled d-orbitals, modifying cation oxidation states, and oxygen or metal cation deficits. These defects change the oxidation state, the electronegativity associated with the material's work function, and the carrier concentration and Fermi levels. The energy level is influenced by oxygen vacancies at the interface of metal oxide. Si oxygen-deficient MoO<sub>3</sub> can be denoted as MoO<sub>3-x</sub> or MoO<sub>x</sub>, where x is the degree of oxygen. After depositing a TMOs layer on Si, oxygen releases free electrons, causing a

defect in the forbidden energy gap near the conduction band and occupying d-orbital states. TMOs with oxygen vacancies are classed as n-type semiconductors, whilst those with metallic vacancies are categorized as p-type semiconductors (Gao M et al., 2018)

### **Importance of passivating contact**

In doped a-Si areas, SHJ solar cells exhibit parasitic absorption and recombination losses. TMO passivated contacts decreased parasitic absorption losses due to the greater bandgap in the emitter zone, recombination loss due to the lack of a strongly doped layer, and functioned as carrier selectivity contacts. The maximum efficiency of 22.1% is achieved when MoO<sub>3-x</sub> is utilised in the hole-contact stack, and 21.1% when TiO<sub>2-x</sub> is used as an electron-selective contact. TMOs with double heterocontact achieved efficiencies of over 23.5%, work functions of 6.9 eV for MoO<sub>x</sub> and ~4.0 eV for TiO<sub>x</sub>, and a  $\eta$  of 24.83% through modelling. TMO connections in solar cells minimize parasitic light absorption while increasing J<sub>sc</sub>, with a high efficiency potential of up to 28.4%.

### **Fermi level pinning effect**

Fermi level pinning (FLP) happens at the metal-semiconductor interface. When metal oxide comes into contact with a Si wafer, the metal's Fermi level matches the c-Si energy levels. This is due to charge transfer between metal and c-Si. The metal's Fermi level is locked at a certain amount of energy within the band gap, resulting in an unequal distribution of charge carriers at the interface. F.L.P. can boost recombination rates and impact device performance. To minimize F.L.P., inserting insulating layers that lower the Schottky barrier height, and hence surface passivation, are used to change energy level alignment and lessen the F.L.P influence on device performance (Ibarra Michel et al., 2023). High doping on silicon surfaces decreases Fermi-level pinning, allowing electrons to interface through dangling bonds or interfacial dipoles, reducing the Schottky barrier that prevents quantum tunnelling (Ibarra Michel et al., 2023). Surface passivation is a method to decrease F.L.P. by adding a thin film of dielectric to the c-Si surface for chemical passivation (Wang, Y et al., 2022). The surface passivation quality is determined through measurements of microwave-reflectance photoconductivity decay (P.C.D.) and photo-reflectance (P.R.), which consider the movement of the Fermi level and changes in energy levels (Essig S et al., 2018; Wong T.K. et al., 2020).

### **Carrier selectivity (hole & electron) & transport mechanisms in TMOs passivating contacts**

Carrier-selectivity is the process by which one carrier out of two is selectively collected by a passivating contact, which is made up of layers that concentrate the conductivity of one carrier and diminish the conductivity of the other. A c-Si solar cell requires significant conductivity asymmetry to operate efficiently. By adjusting surface carrier concentrations and generating asymmetric carrier flows through contact, selectivity is achieved (Essig S et al., 2018). TMOs that lack metal or oxygen cations, which can result in band-gap defects or modifications to the oxidation state of the cations, These defects modify electronegativity, which is directly related to the material work function, and they also impact carrier concentration and push the Fermi level towards one band. TMO materials MoO<sub>3-x</sub>, V<sub>2</sub>O<sub>5-x</sub>, and WO<sub>3-x</sub> have a high work function but lower Fermi levels than Si; when deposited on silicon wafers, their Fermi levels align, inducing band bending in c-Si near the absorber's valence band. A MoO<sub>3</sub>/Si interface permits holes to be carried from Si to TMOs, but electrons cannot be moved because to a higher conduction-band offset (Bhatia et al., 2019). TMOs like TiO<sub>2</sub>, Nb<sub>2</sub>O<sub>5</sub>, Ta<sub>2</sub>O<sub>5</sub>, and ZnO are electron selective contacts have a larger offset in a valence band and a smaller offset in a conduction band with c-Si, electrons can travel through the narrow conduction band (C.B.) while blocking holes in the broader valence band (V.B.) Figure 11 shows the carrier selectivity of TMO contacts. TiO<sub>2</sub> is an electron-selective contact with a wide valence band offset with Si and a narrow conduction band offset, whereas MoO<sub>3</sub> is a hole-selective contact with a larger conduction band offset and a smaller valence band offset, as seen in Figure 15 (Mehmood H et al., 2020 ; Messmer C et al., 2018).

MoO<sub>3</sub>, V<sub>2</sub>O<sub>5</sub>, NiO, and WO<sub>3</sub> are hole-selective contacts with narrower valence band offset and greater conduction offset, allowing holes to pass while blocking electrons from c-Si to TMO materials (Li F et al., 2019; Messmer C et al., 2018), as shown in figure 12. The second prerequisite is that when the TMO's conduction band energy exceeds the Si layer's valence band energy, band-to-band (B2B) tunnelling of surplus holes takes place, and vice versa for TAT, Excess holes tunnel through band-to-band when TMO's conduction band energy exceeds Si layer's valence band energy as shown in figure 13, and traps in TMOs serve as intermediate energy levels, permitting trap-assisted tunnelling through gaps in the valence band to reach the conduction band (Plakhotnyuk et al., 2017).

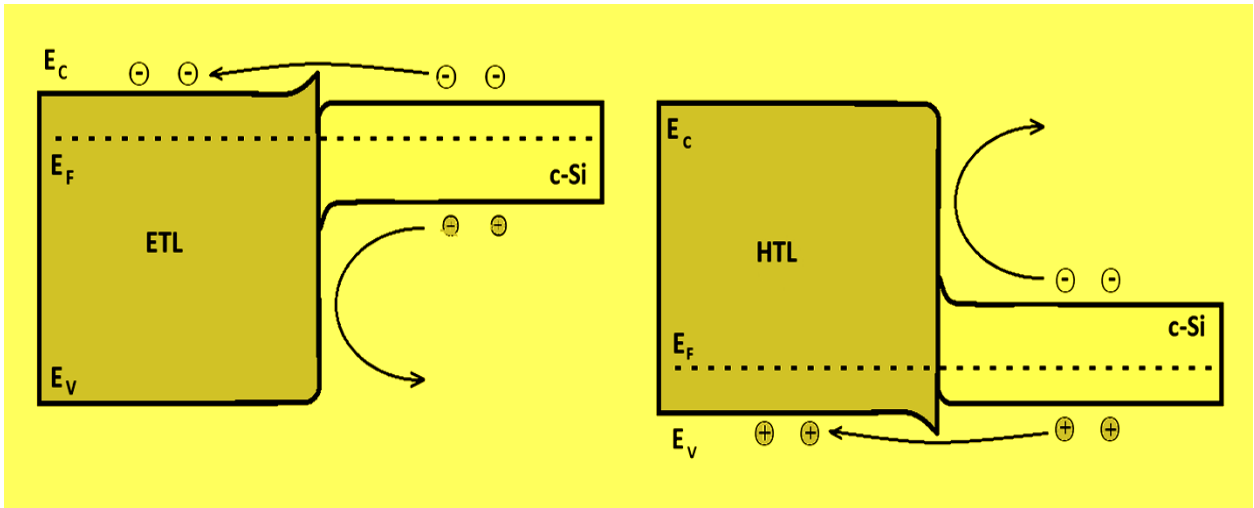


Fig. 12 TMOs hole-selective & electron-selective passivating contacts

Trap-assisted tunnelling is the process by which holes in the valence band are helped to tunnel to the conduction band by the traps in the TMO, which serve as intermediary energy levels as shown in figure 14 (Wang Y et al., 2022; Melskens J. et al., 2018; Hussain S et al., 2019).

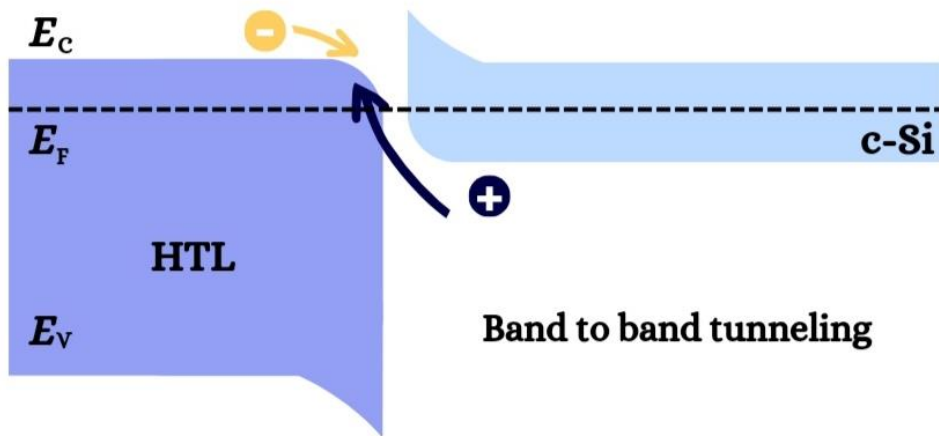


Fig.13 Band to band tunneling for hole

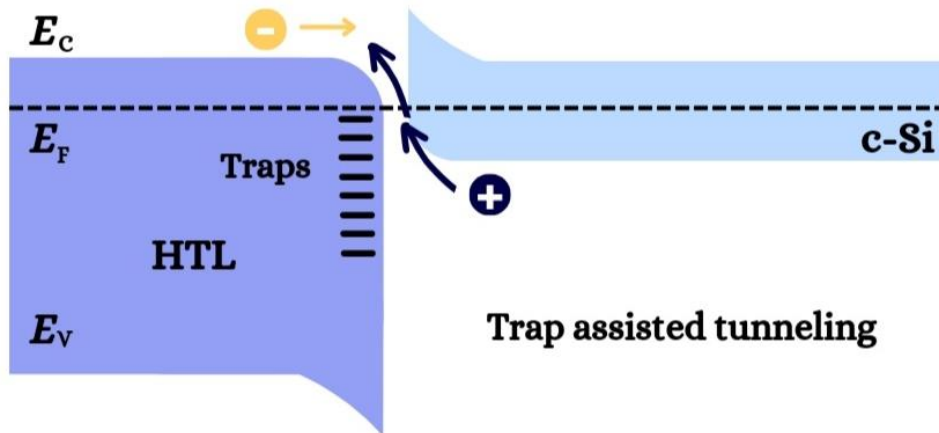


Fig.14 Trap assisted tunneling tunneling for hole

It has been investigated and used to investigate TMOs as electron contacts, such as ZnO, Nb<sub>2</sub>O<sub>5-x</sub>, Ta<sub>2</sub>O<sub>5-x</sub>, and TiO<sub>2-x</sub>. These electron-selective TMOs' precise electrical characteristics may vary depending on stoichiometry and defects

(Acharyya S et al., 2022; Avasthi S et al., 2013). TMO electron-selective contact with c-Si has a narrower conduction band offset, enabling electron transport from Si to TMO, and a greater conduction band offset, blocking hole transport from Si to TMO, as shown in Figure 11 (Wang, Y et al., 2022). TMOs like  $\text{TiO}_2$ ,  $\text{Ta}_2\text{O}_5$ ,  $\text{ZnO}$ ,  $\text{CdO}$ ,  $\text{MgO}$ , and  $\text{Nb}_2\text{O}_5$  have narrower conduction bands and greater valence band offsets, allowing electrons to pass while blocking holes from c-Si to TMO materials. The narrow conduction band and greater valence band offset ranges correspond to 0.051 eV and 2.01 eV, respectively (Wang, Y et al., 2022). TMO materials  $\text{MoO}_3$ -x,  $\text{V}_2\text{O}_5$ -x, and  $\text{WO}_3$ -x have a high work function but lower Fermi levels than Si; when deposited on silicon wafers, their Fermi levels align, inducing band bending in c-Si near the absorber's valence band. A  $\text{MoO}_3$ /Si interface permits holes to be carried from Si to TMOs, but electrons cannot be moved because to a higher conduction-band offset (Bhatia et al., 2019). TMOs like  $\text{TiO}_2$ ,  $\text{Nb}_2\text{O}_5$ ,  $\text{Ta}_2\text{O}_5$ , and  $\text{ZnO}$  are electron selective contacts have a larger offset in a valence band and a smaller offset in a conduction band with c-Si, electrons can travel through the narrow conduction band (C.B.) while blocking holes in the broader valence band (V.B.) Figure 11 shows the carrier selectivity of TMO contacts.  $\text{TiO}_2$  is an electron-selective contact with a wide valence band offset with Si and a narrow conduction band offset, whereas  $\text{MoO}_3$  is a hole-selective contact with a larger conduction band offset and a smaller valence band offset, as seen in Figure 15 (Mehmood H et al., 2020 ; Messmer C et al., 2018).

Passivating contacts reduce contact saturation current ( $J_{0c}$ ) and contact resistivity ( $\rho_c$ ), which represent resistance to the collected carrier and conductivity to the non-collected carrier, respectively (Bivour M et al., 2016; Melskens J. et al., 2018). The carrier selectivity of passivated contact is significantly influenced by the open circuit voltage ( $V_{oc}$ ) (Wang, Y et al., 2022).

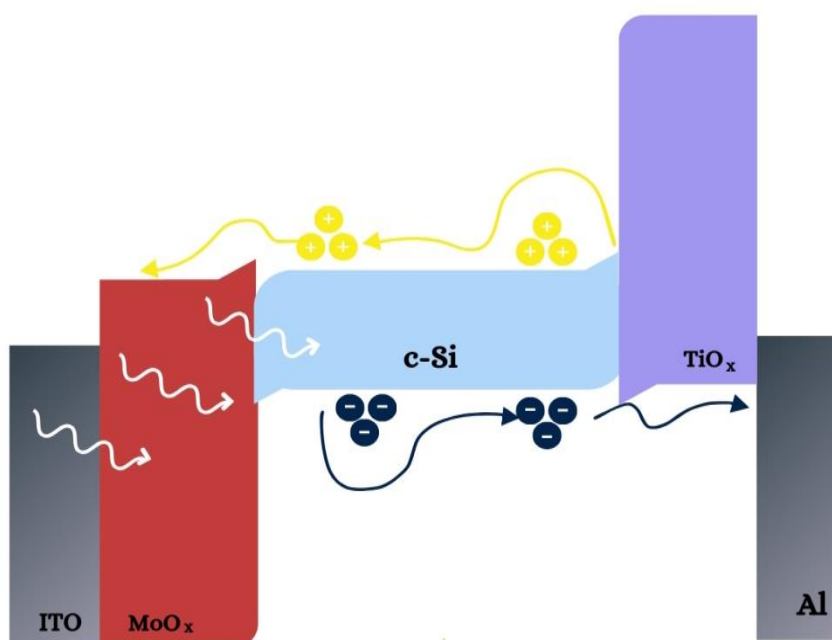
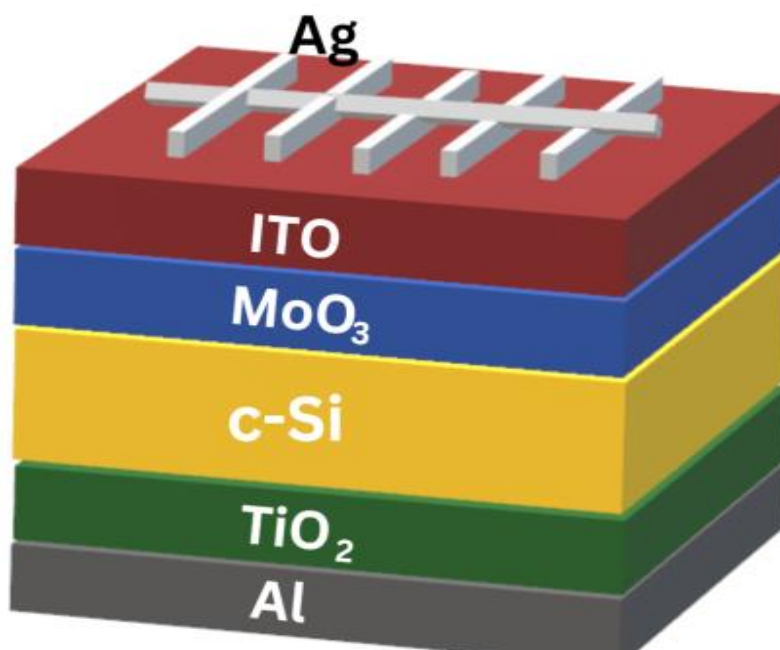


Fig. 15  $\text{TiO}_2$  and  $\text{MoO}_3$  band offset and carrier transport.

#### Novel-design and Fabrication of TMO contact base SHJ solar cell

The novel design of a TMO double heterocontact c-Si solar cell is shown in figure- 16. A doping-free asymmetric double heterocontact passivated c-Si solar cell is made up of an n- or p-type Si wafer with double polishing, 100-degree orientation, and a thickness of less than 250 micrometres. For surface passivation,  $\text{SiO}_2$  layers of about 2 nm thickness are deposited on both sides of the wafer;  $\text{MoO}_3$  layers of about 7 nm thickness are placed on the front side of the wafer; and  $\text{TiO}_2$  layers of about 5 nm thickness are formed on the other sides of the wafer. The front surface is coated with about 80 nm of ITO, which reduces optical losses and improves light absorption. In the bus bar pattern, there is a silver coating on the front 200 nm. TMO double-contact silicon solar cell's novel manufacturing for improving crystalline silicon solar cell performance (Mehmood H et al., 2020 ; Patwardhan S et al., 2021).



**Fig. 16. Design of TMOs double heterocontact solar cells**

#### **Fabrication method**

The c-Si solar cell uses TiO<sub>2</sub> as an electron-selective contact and MoO<sub>3</sub> as a hole-selective contact. Cleaning n-type, Czochralski, or floating silicon wafers using R.C.A. I and R.C.A. II solutions in 2% HF). Thermal evaporator/pulse laser deposition (PLD) or atomic layer deposition (ALD) is used to grow the MoO<sub>3</sub> film on one side while the TiO<sub>2</sub> film is grown on the other. ITO serves as the front surface of the TiO<sub>2</sub> layer, with Al deposited at the rear and Ag at the front. The Si wafer is kept within the chamber during the deposition of material (Patwardhan S. et al., 2021). SiO<sub>2</sub> passivation layer is inherently present on silicon wafers of thickness up to 2 nm after RCA I and RCA II cleaning. SiO<sub>2</sub>/Al<sub>2</sub>O<sub>3</sub> layers of thickness up to 2 nm can be deposited by PLD. When deposition by ALD occurs, tetrakis (*di-methyl-amido*) titanium (*TDMA-Ti*) or titanium tetrachloride (*TiCl<sub>4</sub>*) and water steam are employed as precursors for titanium and oxygen, respectively, at temperatures < 200°C. Ozone and Mo(CO)<sub>6</sub> are used as precursors for molybdenum and oxygen deposition of MoO<sub>3</sub> films on Si wafers. When deposition is done using the pulse laser deposition technique, the material that is being targeted is a silicon substrate in the form of a pellet with a diameter of 1 inch, a thickness of 0.4 cm, and a substrate dimension of 1 cm<sup>2</sup> (Patwardhan S. et al., 2021). Transition metal oxides TiO<sub>2</sub>, MoO<sub>3</sub>, and ITO are deposited on silicon wafers by pulse laser deposition technique (using a KrF excimer laser at 248 nm for 20 ns) with thicknesses ranging from 05 nm to 10 nm. TiO<sub>2</sub> of thickness 5 nm is deposited on one side of the silicon wafer at a substrate temperature of 500°C, base-pressure 10<sup>-6</sup> Torr, an oxygen partial pressure of 35 mTorr, laser energy of 250 mJ/cm<sup>2</sup>, a repetition rate of 6 Hz, and a deposition time of 5 minutes. MoO<sub>3</sub> is deposited on the other side of the silicon wafer at a substrate temperature of 500°C at a pressure of 10<sup>-6</sup> Torr, oxygen partial pressure of 0.1 mTorr, laser energy of 250 mJ/cm<sup>2</sup>, and a repetition rate of 5 Hz for 6 minutes (Scire, D. et al., 2018). ITO thin films are grown by P.L.D. or RF sputtered on a silicon substrate at a temperature of 200°C and 10 mTorr of oxygen pressure. The optimum thickness of the ITO is 80 nm. A silver coating on the front surface of 200 nm is deposited with a bus-bar and finger pattern, and a rare surface Al coating of 200 nm has been done (Mehmood H et al., 2020). The thickness is measured by a depth profilometer. The characterization of the sample by XRD, AFM, and solar simulator with the Keithley four probe method for I-V measurement to find the efficiency of solar cells using the solar cell parameters FF, J<sub>sc</sub>, and V<sub>oc</sub> (Liu Y et al., 2020). HBC structure (SHJ-IBC) like TMOs contact base SHJ-IBC structure can be developed for c-Si solar cells with high efficiency.

#### **Challenges and future research opportunities**

**The challenges** in silicon solar cell manufacturing are as follows:

In order to rival fossil fuels, it's vital to reduce costs in raw materials, production processes, and balance-of-system components from non-traditional sources (Liu Y et al., 2020 ). Thin-film technologies and new cell architectures have the potential to improve the effectiveness of silicon solar cells, but they are still expensive (Ibarra Michel et al., 2023). The use of hazardous chemicals in manufacturing necessitates the adoption of cleaner production methods, waste reduction, and recycling (Wang, Y et al., 2022 ). Solar panels require long-term durability and reliability for maximum energy yield, and large areas of land or rooftop space may be required for production of electric energy. Metal coating the front and back surfaces of silver and aluminium on a silicon wafer is costly and difficult to achieve excellent conductivity. The challenge of creating an ultra-thin dielectric layer is a major one. Solar cell manufacture is expensive, which makes commercialization difficult. Experimental technologies cannot directly determine electron or hole-selective contact.

Solar cells do not function at night or during cloudy or rainy seasons, resulting in lower power output. In some cases, the storage batteries or systems are expensive and unsustainable. Silicon-crystalline wafer modules are heavier and occupy a



larger roof and area. Future prospects for c-Si solar cells include the following: The study focuses on improving Technology for c-Si solar cells to increase efficiency, reduce costs, long-term reliability and improve sustainability. It includes exploring advanced cell topologies, passivated contacts, light trapping strategies, new cell and module designs, passivation strategies, surface texturing, clean production methods, and recycling and recovery of silicon components to decrease recombination losses and reflection while increasing light absorption (Chang, N.L et al., 2023 ). Perovskite solar cells possess the capability to surpass traditional silicon efficiency limits. Future research should focus on improving stability, scalability, and manufacturing processes. Tandem solar cells, which combine multiple materials with complementary absorption spectra, have potential for higher efficiencies. Future research should focus on optimizing design and fabrication techniques, exploring new materials, and improving efficiency.

Metal coating the front and back surfaces of silver and aluminium on a silicon wafer is costly and difficult to achieve excellent conductivity. The challenge of creating an ultra-thin dielectric layer is a major one. Solar cell manufacture is expensive, which makes commercialization difficult. Experimental technologies cannot directly determine electron or hole-selective contact. Solar cells do not function at night or during cloudy or rainy seasons, resulting in lower power output. In some cases, the storage batteries or systems are expensive and unsustainable.

Silicon-crystalline wafer modules are heavier and occupy a larger roof and area. Advancements in characterization techniques like electron microscopy, spectroscopy, and carrier lifetime measurements offer insights into crystalline silicon solar cells' material properties and performance limitations. Research on sustainable manufacturing processes, eco-friendly materials, and recycling technologies is crucial for reducing the environmental impact of solar cell manufacturing and end-of-life disposal (Geissbühler, J et al., 2015).

Quinone, an organic battery storing sunlight energy for a few days, and rechargeable lithium-oxygen batteries for electronic vehicles are potential solutions to reduce renewable energy costs (Chang, N.L et al., 2023; Sharma shruti et al., 2015 ).

In future scope the hybrid solar cells are emerging, using poly-Si contact technology and TMOs using MoO<sub>x</sub> in traditional SHJ cells rather than a-Si(p):H. Passivating contacts are crucial for enhancing efficiencies beyond 26.7% in IBC cells, simplifying the fabrication process. Utilizing rear-asymmetric connections and front sided diffused contacts, hybrid SHJ solar cells integrate field-passivated IBCs with successful SHJs (Liu Y et al., 2020).

Superior passivation capabilities are exhibited by TMOs asymmetric heterocontact silicon solar cells due to wide bandgap contact materials. Various silicon solar cell technologies, including MoO<sub>x</sub> full-area back contacts (Hussain S et al., 2019) IBC designs, monofacial DASH with TMO-based passivation, monofacial and bifacial SHJ, IBC-POLO, and TOPCon structures, have been reviewed for industrial prospects. Product design is crucial in commercial applications like floating solar farms and building integrated photovoltaic's (BIPV) which save land and allow natural light in homes and offices (Deshpande R.A. et al.,; 2021 Melskens J. et al., 2018; Sharma S et al., 2015).

## CONCLUSION

Crystalline silicon (c-Si) solar cells are a sustainable, long-term, and environmentally friendly renewable energy source that dominates 95% of the global electricity market. Photovoltaic (PV) technology converts solar energy into electrical energy, which is clean, pollution-free, noiseless, and has high energy quality. This review paper discusses the fundamentals of solar cells, including their mechanism of operation and design factors, their types, passivating contacts, and various solar cell structure technologies. The study aims to improve c-Si solar cell technology by exploring advanced cell topologies, passivating contacts, light trapping strategies, new cell and module designs, passivation strategies, surface texturing, clean production methods, and recycling and recovery of silicon components. Perovskite solar cells possess the capability to surpass traditional silicon efficiency limits, and future research should focus on improving stability, scalability, and manufacturing processes. Tandem solar cells, thin-film solar cells, and nanostructured materials are also being explored. For the performance improvement of c-Si solar cells, it is crucial to focus on improving their passivation and efficiency. Doped a-Si:H based carrier selective contact faces loss mechanisms like parasitic absorption and defect-assisted recombination, but alternative doping-free designs like TOPCon structures, novel IBC-SHJ (H.B.C.) structures, and field-effect passivated I.B.C. architectures show industrial potential. New technologies have improved solar cell efficiency, with SHJ-IBC called HBC cells achieving 26.7% efficiency with significant improvements due to passivated contacts. However, these structures remain expensive due to their optical enhancement strategies and gadget conceptions. Subsequent investigations seek to reduce thermal expansion mismatches and wafer thickness and implement various module sizes and technologies to support cost reductions in photovoltaic energy.

Interdigitated back-contact solar cells offer high efficiency, but their complex structure and high-cost manufacturing process may limit their application domain. The carrier-selective TMO passivated contacts are essential for reducing recombination and resistance losses. In this review, we have discussed the charge carrier transport mechanism, electron and hole carrier selectivity, material property optimization, the difficulties and potential of TMOs connections, and optimizing the TMOs contact energy band with c-Si. It is possible to create TMOs that have dopant-free carrier-selective contacts utilizing a simple process at low temperatures without the emission of hazardous and flammable gases. Further optimization of hole and electron selective contact with c-Si data can help find the appropriate combination of electron and hole carrier selective contacts. TMO asymmetric hetero-contact solar cells can achieve efficiencies of MoO<sub>3</sub> as hole-picking and TiO<sub>2</sub> as electron-picking contact of around 23.5%, while TMO double-asymmetric hetero-contact/passivated contacts in c-Si solar cells have an efficiency of 24.83% and a further potential of more than 28.4%. Doping-free concepts like molybdenum oxide are being

explored to reduce Auger recombination in carrier-selective regions. Short-term research aims to reduce manufacturing costs by using thinner wafers and developing thermal processing methods. In order to be competitive, solar technology needs to surpass 23% module efficiency at a cost of less than US\$0.2/W within the next five years, as crystalline silicon currently holds a dominant market share.

The price per watt of solar power equipment is crucial due to the growing availability of renewable resources appropriate for home or small-scale solar energy requirements. The levelized cost of electricity is a key factor in comparing cost vs. output power, with the higher cell efficiency of a doping-free asymmetric heterocontact solar cell indicating potential as a promising renewable energy source. The next step should be to optimise current carrier-selective substances and contact architectures by employing novel contact and interfacial passivation substances, cost-effective deposition processes, and unique device designs like TMO-based SHJ-IBC, including fully interdigitated back-contact and TMO passivated contacts (TMO) for c-Si solar cells, which have generated interest and the potential to lower manufacturing expenses and, as a result, provide a levelized cost of energy (LCOE) to our society with eco-friendliness in the era of global warming.

## ACKNOWLEDGEMENTS

The research is not supported by any Government, agency of technology, and at Poornima University, the university fee for the Ph.D. course has to be deposited by the research scholar.

**Authors' contributions:** The corresponding author prepares the entire manuscript and collect the information, whereas the second author helped in collect the information and guided the writing of this article. The authors read and approved the final manuscript.

**Funding:** There is no funding granted by any agency or university. Research work is being done in the institution's laboratory, where a fee is deposited by the researcher per year.

**Availability of data and materials:** As this is a review article, no information has been generated in the laboratory; instead, gather those from various sources and declare that all were collected by the researcher at the laboratory / library of the Poornima University, Jaipur, India.

## Declarations

**Competing interests:** The authors declare that they have no competing interests.

## REFERENCES:

1. Acharyya, S., Sadhukhan, S., Panda, T., Ghosh, D.K., Mandal, N.C., Nandi, A., Bose, S., Das, G., Maity, S., Chaudhuri, P., and Saha, H., 2022. Dopant-free materials for carrier-selective passivating contact solar cells: A review. *Surfaces and Interfaces*, 28, p. 101687. <https://doi.org/10.1016/j.surfin.2021.101687>
2. Al-Ezzi, A.S., and Ansari, M.N.M., 2022. Photovoltaic solar cells: a review. *Applied System Innovation*, 5(4), p. 67. <https://doi.org/10.3390/asi5040067>
3. Allen, T.G., Bullock, J., Yang, X., Javey, A., and De Wolf, S., 2019. Passivating contacts for crystalline silicon solar cells. *Nature Energy*, 4(11), pp. 914–928, <https://doi.org/10.1038/s41560-019-0463-6>
4. Almora, O., Gerling, L.G., Voz, C., Alcubilla, R., Puigdollers, J., and Garcia-Belmonte, G., 2017. Superior performance of V2O5 as hole-selective contact over other transition metal oxides in silicon heterojunction solar cells. *Solar Energy Materials and Solar Cells*, 168, pp. 221–226.
5. Avasthi, S., McClain, W.E., Man, G., Kahn, A., Schwartz, J., and Sturm, J.C., 2013. Hole-blocking titanium-oxide/silicon heterojunction and its application to photovoltaics. *Applied Physics Letters*, 102(20).
6. Badawy, W.A., 2015. A review of solar cells, from single crystals to porous materials and quantum dots. *Journal of Advanced Research*, 6(2), pp. 123–132. <https://doi.org/10.1016/j.jare.2013.10.001>
7. Ballif, C., Haug, F.J., Boccard, M., Verlinden, P.J., and Hahn, G., 2022. Status and perspectives of crystalline silicon photovoltaics in research and industry. *Nature Reviews Materials*, 7(8), pp. 597–616, <https://doi.org/10.1038/s41578-022-00423-2>
8. Battaglia, C., Cuevas, A., and De Wolf, S. (2016). High-efficiency crystalline silicon solar cells: status and perspectives. *Energy & Environmental Science*, 9(5), pp. 1552–1576. DOI: 10.1039/c5ee03380b
9. Bhatia, S., Khorakiwala, I.M., Markose, K.K., Nair, P.R., and Antony, A., 2019. MoO<sub>3</sub> as hole-selective contact for diffusion-free solar cells. In *The Physics of Semiconductor Devices: Proceedings of IWPSD 2017* (pp. 329–333). Springer International Publishing. [https://doi.org/10.1007/978-3-319-97604-4\\_50](https://doi.org/10.1007/978-3-319-97604-4_50).
10. Bivour M., Zähringer F., Ndione P., and Hermle M. sputter-deposited WO<sub>x</sub> and MoO<sub>x</sub> for hole-selective contacts. *Energy Procedia*. 2017; 124:400–405. doi:10.1016/j.egypro.2017.09.259.
11. Bullock J, Wan Y, Hettick M, et al., Dopant-free partial rear contacts enable 23% silicon solar cells. *Adv Energy Mater*. 2019;9(9):1803367. doi:10.1002/aenm.201803367
12. Bullock, J., Cuevas, A., Allen, T., and Battaglia, C., 2014. Molybdenum oxide (MoO<sub>x</sub>): A versatile hole contact for silicon solar cells. *Applied Physics Letters*, 105(23).
13. Bullock, J., Hettick, M., Geissbühler, J., Ong, A.J., Allen, T., Sutter-Fella, C.M., Chen, T., Ota, H., Schaler, E.W., De Wolf, S., and Ballif, C., 2016. Efficient silicon solar cells with dopant-free asymmetric heterocontacts. *Nature Energy*, 1(3), pp. 1–7. doi:10.1038/nenergy.2015.31

14. Bullock, J., Wan, Y., Xu, Z., Essig, S., Hettick, M., Wang, H., Ji, W., Boccard, M., Cuevas, A., Ballif, C., and Javey, A., 2018. Stable dopant-free asymmetric heterocontact silicon solar cells with efficiencies above 20%. *ACS Energy Letters*, 3(3), pp. 508–513.
15. Chander, S., and Tripathi, S.K., 2022. Recent advancements in efficient metal oxide-based flexible perovskite solar cells: a short review. *Materials Advances*, 3(19), pp. 7198–7211.
16. Chang, N.L., Poduval, G.K., Sang, B., Khoo, K., Woodhouse, M., Qi, F., Dehghanimadvar, M., Li, W.M., Egan, R.J., and Hoex, B., 2023. Techno-economic analysis of the use of atomic layer-deposited transition metal oxides in silicon heterojunction solar cells. *Progress in Photovoltaics: Research and Applications*, 31(4), pp. 414–428.
17. Chee, K.W., Ghosh, B.K., Saad, I., Hong, Y., Xia, Q.H., Gao, P., Ye, J., and Ding, Z.J., 2022. Recent advancements in carrier-selective contacts for high-efficiency crystalline silicon solar cells: an industrially evolving approach. *Nano Energy*, 95, p. 106899. <https://doi.org/10.1016/j.nanoen.2021.106899>
18. Chowdhury, S., Kumar, M., Dutta, S., Park, J., Kim, J., Kim, S., Ju, M., Kim, Y., Cho, Y., Cho, E.C., and Yi, J., 2019. High-efficiency crystalline silicon solar cells: a review. *Energy*, 15(3), pp. 36–45. <https://doi.org/10.7849/ksnre.2019.3.15.3.036>.
19. ., 2021. Advances in solar cell technology: An overview. *J. Sci. Res*, 65(02), pp.72-75. DOI: 10.37398/JSR.2021.650214
20. Dhar, A., Ahmad, G., Pradhan, D., and Roy, J.N., 2020. Performance analysis of a c-Si heterojunction solar cell with passivated transition metal oxide carrier-selective contacts. *Journal of Computational Electronics*, 19, pp. 875–883.
21. Dréon J, Jeangros Q, Cattin J, et al., 2020. 23.5%-efficient silicon heterojunction silicon solar cell using molybdenum oxide as hole-selective contact. *Nano Energy*, 70:104495. doi:10.1016/j.nanoen.2020.104495.
22. Essig, S., Dréon, J., Rucavado, E., Mews, M., Koida, T., Boccard, M., Werner, J., Geissbühler, J., Löper, P., Morales-Masis, M., and Korte, L., 2018. Towards annealing-stable molybdenum-oxide-based hole-selective contacts for silicon photovoltaics. *Solar RRL*, 2(4), p. 1700227.
23. Flathmann, C., Meyer, T., Titova, V., Schmidt, J., and Seibt, M., 2023. Composition and electronic structure of SiO<sub>x</sub>, TiO<sub>y</sub>, and Al passivating carrier selective contacts on n-type silicon solar cells. *Scientific Reports*, 13(1), p. 3124. <https://doi.org/10.1038/s41598-023-29831-2>
24. Gao M, Chen D, Han B, et al., Bifunctional hybrid a-SiO<sub>x</sub>(Mo) layer for hole-selective and interface passivation of highly efficient MoO<sub>x</sub>/a-SiO<sub>x</sub>(Mo)/n-Si heterojunction photovoltaic device. *ACS Appl Mater Interfaces*. 2018;10(32):27454-27464. doi:10.1021/acsami.8b07001.
25. García-Hernansanz R, García-Hemme E, Montero D, et al., Transport mechanisms in silicon heterojunction solar cells with molybdenum oxide as a hole transport layer. *Sol Energy Mater Sol Cells*. 2018;185: 61–65. doi:10.1016/j.solmat.2018.05.019.
26. García-Hernansanz, R., Pérez-Zenteno, F., Duarte-Cano, S., Caudevilla, D., Algaidy, S., García-Hemme, E., Olea, J., Pastor, D., Del Prado, A., San Andrés, E., and Mártel, I., 2023. Inversion Charge Study in TMO Hole-Selective Contact-Based Solar Cells. *IEEE Journal of Photovoltaics*.
27. Geissbühler, J., Werner, J., Martin de Nicolas, S., Barraud, L., Hessler-Wyser, A., Despeisse, M., Nicolay, S., Tomasi, A., Niesen, B., De Wolf, S., and Ballif, C., 2015. 22.5% efficient silicon heterojunction solar cell with molybdenum oxide hole collector. *Applied Physics Letters*, 107(8).
28. Gerling, L.G., Mahato, S., Morales-Vilches, A., Masmitja, G., Ortega, P., Voz, C., Alcubilla, R., and Puigdollers, J., 2016. Transition metal oxides as hole-selective contacts in silicon heterojunction solar cells. *Solar Energy Materials and Solar Cells*, 145, pp. 109–115.
29. Gerling, L.G., Voz, C., Alcubilla, R., and Puigdollers, J., 2017. Origin of passivation in hole-selective transition metal oxides for crystalline silicon heterojunction solar cells. *Journal of Materials Research*, 32, pp. 260–268.
30. Gregory, G., Luderer, C., Ali, H., Sakthivel, T.S., Jurca, T., Bivour, M., Seal, S., and Davis, K.O., 2020. Spatial atomic layer deposition of molybdenum oxide for industrial solar cells. *Advanced Materials Interfaces*, 7(22), p. 2000895.
31. Green MA. The passivated emitter and rear cell (PERC): from conception to mass production. *Sol Energy Mater Sol Cells*. 2015;143: 190–197. doi:10.1016/j.solmat.2015.06.055.
32. Greiner MT, Chai L, Helander MG, Tang W-M, and Lu Z-H. Transition metal oxide work functions: the influence of cation oxidation state and oxygen vacancies. *Adv Funct Mater*. 2012;22(21):4557–4568. doi:10.1002/adfm.201200615
33. Greiner MT, Chai L, Helander MG, Tang W-M, and Lu Z-H. Metal/metaloxide interfaces: how metal contacts affect the work function and band structure of MoO<sub>3</sub>. *Adv Funct Mater*. 2013;23(2):215-226. doi:10.1002/adfm.201200993
34. Hussain, S.Q., Mallem, K., Khan, M.A., Khokhar, M.Q., Lee, Y., Park, J., Lee, K.S., Kim, Y., Cho, E.C., Cho, Y.H., and Yi, J., 2019. Versatile hole carrier selective MoO<sub>x</sub> contact for high-efficiency silicon heterojunction solar cells: A review. *Transactions on Electrical and Electronic Materials*, 20, pp. 1–6.
35. Hussain, S.Q., Mallem, K., Kim, Y.J., Le, A.H.T., Khokhar, M.Q., Kim, S., Dutta, S., Sanyal, S., Kim, Y., Park, J., and Lee, Y., 2019. Ambient annealing influences surface passivation and stoichiometric analysis of the molybdenum oxide layer for carrier-selective contact solar cells. *Materials Science in Semiconductor Processing*, 91, pp. 267–274.
36. Ibarra Michel, J., Dréon, J., Boccard, M., Bullock, J., and Mocco, B., 2023. Carrier-selective contacts using metal compounds for crystalline silicon solar cells. *Progress in Photovoltaics: Research and Applications*, 31(4), pp. 380–413. <https://doi.org/10.1002/pip.3552>
37. Imran, H., Abdolkader, T.M., and Butt, N.Z., 2016. Carrier-selective NiO/Si and TiO<sub>2</sub>/Si contacts for silicon heterojunction solar cells. *IEEE Transactions on Electron Devices*, 63(9), pp. 3584–3590.

38. Jhaveri, J., Berg, A.H., and Sturm, J.C., 2018. Isolation of hole versus electron current at p-Si/TiO<sub>2</sub> selective contact using a heterojunction bipolar transistor structure. *IEEE Journal of Photovoltaics*, 8(3), pp. 726–732.
39. Kang, D., Ko, J., Lee, C., Kim, D., Lee, H., Kang, Y., and Lee, H.S., 2023. Titanium oxide nanomaterials as an electron-selective contact in silicon solar cells for photovoltaic devices. *Discover Nano*, 18(1), p. 39.
40. Khokhar, M.Q., Hussain, S.Q., Chowdhury, S., Zahid, M.A., Pham, D.P., Jeong, S., Kim, S., Cho, E.C., and Yi, J., 2022. High-efficiency hybrid solar cell with a nano-crystalline silicon oxide layer as an electron-selective contact. *Energy Conversion and Management*, 252, p. 115303. <https://doi.org/10.1016/j.enconman.2021.115033>.
41. Kumari, J., Basumatary, P., Gangwar, M.S. and Agarwal, P., 2021. Molybdenum oxide (MoO<sub>3-x</sub>) as an emitter layer in silicon based heterojunction solar cells. *Materials Today: Proceedings*, 39, pp.1996-1999. <https://doi.org/10.1016/j.matpr.2020.08.527>
42. Kodati, R.B. and Rao, P.N., 2020. A review of solar cell fundamentals and technologies. *Advanced Science letters*, 26.
43. Koswatta, P., Boccard, M. and Holman, Z., 2015, June. Carrier-selective contacts in silicon solar cells. In 2015 IEEE 42nd photovoltaic specialist conference (PVSC) (pp. 1-4). IEEE. DOI: 10.1109/PVSC.2015.7356143.
44. Le, A.H.T., Dréon, J., Michel, J.I., Boccard, M., Bullock, J., Borojevic, N. and Hameiri, Z., 2022. Temperature-dependent performance of silicon heterojunction solar cells with transition-metal-oxide-based selective contacts. *Progress in Photovoltaics: Research and Applications*, 30(8), pp.981- 993.
45. Li, F., Sun, Z., Zhou, Y., Wang, Q., Zhang, Q., Dong, G., Liu, F., Fan, Z., Liu, Z., Cai, Z. and Zhou, Y., 2019. Lithography-free and dopant-free back-contact silicon heterojunction solar cells with solution-processed TiO<sub>2</sub> as the efficient electron selective layer. *Solar Energy*.
46. Lin, H., Yang, M., Ru, X., Wang, G., Yin, S., Peng, F., Hong, C., Qu, M., Lu, J., Fang, L. and Han, C., 2023. Silicon heterojunction solar cells with up to 26.81% efficiency achieved by electrically optimized nanocrystalline-silicon hole contact layers. *Nature Energy*, pp.1-11.
47. Liu, J., Yao, Y., Xiao, S. and Gu, X., 2018. Review of status developments of high-efficiency crystalline silicon solar cells. *Journal of Physics D: Applied Physics*, 51(12), p.123001. <https://doi.org/10.1088/1361-6463/aaac6d>
48. Liu, Y., Li, Y., Wu, Y., Yang, G., Mazzarella, L., Procel-Moya, P., Tamboli, A.C., Weber, K., Boccard, M., Isabella, O. and Yang, X., 2020. High-efficiency silicon heterojunction solar cells: materials, devices and applications. *Materials Science and Engineering: R: Reports*, 142, p.100579.
49. Mallem, K., Kim, Y.J., Hussain, S.Q., Dutta, S., Le, A.H.T., Ju, M., Park, J., Cho, Y.H., Kim, Y., Cho, E.C. and Yi, J., 2019. Molybdenum oxide: A superior hole extraction layer for replacing p-type hydrogenated amorphous silicon with high efficiency heterojunction Si solar cells. *Materials Research Bulletin*, 110, pp.90-96.
50. Martín, I., López, G., Garín, M., Ros, E., Ortega, P., Voz, C. and Puigdollers, J., 2023. Hole selective contacts based on transition metal oxides for c-Ge thermophotovoltaic devices. *Solar Energy Materials and Solar Cells*, 251, p.112156.
51. Masmitjà G, Ortega P, Puigdollers J, et al., 2018. Interdigitated backcontacted crystalline silicon solar cells with low-temperature dopant-free selective contacts. *J Mater Chem A*. 2018;6(9): 3977-3985. doi:10.1039/C7TA11308K
52. Masmitjà, G., Ros, E., Almache-Hernández, R., Pusay, B., Martín, I., Voz, C., Saucedo, E., Puigdollers, J. and Ortega, P., 2022. Interdigitated back-contacted crystalline silicon solar cells fully manufactured with atomic layer deposited selective contacts. *Solar Energy Materials and Solar Cells*, 240, p.111731.
53. Mehmood, H., Nasser, H., Tauqeer, T. and Turan, R., 2020. Numerical analysis of dopant-free asymmetric silicon heterostructure solar cell with SiO<sub>2</sub> as passivation layer. *International Journal of Energy Research*, 44(13), pp.10739-10753.
54. Mehmood, H., Nasser, H., Tauqeer, T. and Turan, R., 2019. Simulation of silicon heterostructure solar cell featuring dopant-free carrier-selective molybdenum oxide and titanium oxide contacts. *Renewable energy*, 143, pp.359-367. <https://doi.org/10.1016/j.renene.2019.05.007>
55. Mehmood, H., Nasser, H., Tauqeer, T., Hussain, S., Ozkol, E. and Turan, R., 2018. Simulation of an efficient silicon heterostructure solar cell concept featuring molybdenum oxide carrier-selective contact. *International Journal of Energy Research*, 42(4), pp.1563-1579.
56. Melskens, J., van de Loo, B.W., Macco, B., Black, L.E., Smit, S. and Kessels, W.M.M., 2018. Passivating contacts for crystalline silicon solar cells: From concepts and materials to prospects. *IEEE Journal of Photovoltaics*, 8(2), pp.373-388.
57. Messmer C, Bivour M, Schön J, Hermle M. Requirements for efficient hole extraction in transition metal oxide-based silicon heterojunction solar cells. *J Appl Phys*. 2018;124(8):085702. doi:10.1063/1.5045250
58. Nayak, M., Mandal, S., Pandey, A., Mudgal, S., Singh, S. and Komarala, V.K., 2019. Nickel oxide hole-selective heterocontact for silicon solar cells: role of SiO<sub>x</sub> interlayer on device performance. *Solar RRL*, 3(11), p.1900261. doi:10.1002/solr.201900261.
59. Parashar PK, Komarala VK. Sputter deposited sub-stoichiometric MoO<sub>x</sub> thin film as hole-selective contact layer for silicon based heterojunction devices. *Thin Solid Films*. 2019;682:76-81. doi:10.1016/j.tsf.2019.05.004
60. Patwardhan, S., Maurya, S., Kumar, A. and Kavaipatti, B., amorphous silicon-free metal-oxides based carrier-selective contacts to crystalline silicon solar cells(2021).
61. Plakhotnyuk, M.M., Schüler, N., Shkodin, E., Vijayan, R.A., Masilamani, S., Varadharajaperumal, M., Crovetto, A. and Hansen, O., 2017. Surface Title passivation and carrier selectivity of the thermal-atomic-layer-deposited TiO<sub>2</sub> on crystalline silicon. *Japanese Journal of Applied Physics*, 56(8S2), p.08MA11.
62. Richter A, Müller R, Benick J, et al., Design rules for high-efficiency both-sides-contacted silicon solar cells with balanced charge carrier transport and recombination losses. *Nat Energy*. 2021;6(4):429-438. doi:10.1038/s41560-021-00805-w

63. Richter A, Benick J, Feldmann F, Fell A, Hermle M, Glunz SW. nType Si solar cells with passivating electron contact: Identifying sources for efficiency limitations by wafer thickness and resistivity variation. *Sol Energy Mater Sol Cells*. 2017;173:96-105. doi:10.1016/J.SOLMAT.2017.05.042
64. Richter, A., Glunz, S.W., Werner, F., Schmidt, J. and Cuevas, A., 2012. Improved quantitative description of Auger recombination in crystalline silicon. *Physical review B*, 86(16), p.165202.
65. Sagar, R. and Rao, A., 2020. Increasing the silicon solar cell efficiency with transition metal oxide nano-thin films as anti-reflection coatings. *Materials Research Express*, 7(1), p.016433.
66. Sanyal, S., Dutta, S., Ju, M., Mallem, K., Panchanan, S., Cho, E.C., Cho, Y.H. and Yi, J., 2019. Hole Selective Contacts: A Brief Overview. *Current Photovoltaic Research*, 7(1), pp.9-14.
67. Schmidt, J., Peibst, R. and Brendel, R., 2018. Surface passivation of crystalline silicon solar cells: Present and future. *Solar Energy Materials and Solar Cells*, 187, pp.39-54.
68. Scire, D., Macaluso, R., Mosca, M., Casaletto, M.P., Isabella, O., Zeman, M. and Crupi, I., 2022. Density of states characterization of TiO<sub>2</sub> films deposited by pulsed laser deposition for heterojunction solar cells. *Nano Research*, 15(5), pp.4048-4057.
69. Shockley, W. and Queisser, H., 2004. Detailed balance limit of efficiency of p–n junction solar cells. In *Renewable Energy* (pp. Vol2\_35-Vol2\_54).
70. Sharma, S., Jain, K.K. and Sharma, A., 2015. Solar cells: in research and applications—a review. *Materials Sciences and Applications*, 6(12), pp.1145-1155. DOI: 10.4236/msa.2015.612113
71. Sopian, K., Cheow, S.L. and Zaidi, S.H., 2017, September. An overview of crystalline silicon solar cell technology: Past, present, and future. In *AIP Conference Proceedings* (Vol. 1877, No. 1). AIP Publishing. <https://doi.org/10.1063/1.4999854>
72. Sui, M., Chu, Y. and Zhang, R., 2021, May. A review of technologies for high efficiency silicon solar cells. In *Journal of Physics: Conference Series* (Vol. 1907, No. 1, p. 012026). IOP Publishing. doi:10.1088/1742-6596/1907/1/012026
73. Tyagi A., Biswas, J., Ghosh, K., Kottantharayil, A. and Lodha, S., 2021. Performance analysis of silicon carrier selective contact solar cells with ALD MoO<sub>x</sub> as hole selective layer. *Silicon*, pp.1-8.
74. V. Titova, J. Schmidt, Selectivity of TiO<sub>x</sub>-based electron-selective contacts on ntype crystalline silicon and solar cell efficiency potential, *Phys. Status Solidi - Rapid Res. Lett.* 15 (9) (2021) 1–8, <https://doi.org/10.1002/pssr.202100246>.
75. Vijayan, R.A., Masilamani, S., Kailasam, S., Shivam, K., Deenadhayalan, B. and Varadharajaperumal, M., 2019. Study of surface passivation and charge transport barriers in DASH solar cell. *IEEE Journal of Photovoltaics*, 9(5), pp.1208-1216.
76. Wang, Y., Zhang, S.T., Li, L., Yang, X., Lu, L. and Li, D., 2023. Dopant-free passivating contacts for crystalline silicon solar cells: Progress and prospects. *EcoMat*, 5(2), p.e12292. <https://doi.org/10.1002/eom2.12292>
77. Wang, Z., Li, P., Liu, Z., Fan, J., Qian, X., He, J., Peng, S., He, D., Li, M. and Gao, P., 2019. Hole selective materials and device structures of heterojunction solar cells: Recent assessment and future trends. *APL Materials*, 7(11).
78. Wong, T.K. and Pei, K., 2022, July. Double Heterojunction Crystalline Silicon Solar Cells: From Doped Silicon to Dopant-Free Passivating Contacts. Author In *Photonics* (Vol. 9, No. 7, p. 477). MDPI. <https://doi.org/10.3390/photonics9070477>.
79. Wolf S De, A. Descoedres, Z. C. Holman, and C. Ballif, “High-efficiency Silicon Heterojunction Solar Cells: A Review,” *Green*, vol. 2, no. 1, pp. 7–24, Jan. 2012.
80. Wong T.K. and Pei, K., 2022, July. Double Heterojunction Crystalline Silicon Solar Cells: From Doped Silicon to Dopant-Free Passivating Contacts. In *Photonics* (Vol. 9, No. 7, p. 477). MDPI. <https://doi.org/10.3390/photonics9070477>
81. Wu W, Lin W, Zhong S, et al., 22% efficient dopant-free interdigitated back contact silicon solar cells. *AIP Conf Proc*. 2018;1999(1): 040025. doi:10.1063/1.5049288.
82. Yan, D., Cuevas, A., Stuckelberger, J., Wang, E.C., Phang, S.P., Kho, T.C., Michel, J.I., Macdonald, D. and Bullock, J., 2023. Silicon solar cells with passivating contacts: Classification and performance. *Progress in Photovoltaics: Research and Applications*, 31(4), pp.310-326. <https://doi.org/10.1002/pip.3574>.
83. Yang X, Bi Q, Ali H, Davis K, Schoenfeld WV, Weber K. HighPerformance TiO<sub>2</sub> -Based Electron-Selective Contacts for Crystalline Silicon Solar Cells. *Adv Mater*. 2016;28(28):5891-5897. doi:10.1002/adma.201600926.
84. Yang X, Zheng P, Bi Q, Weber K. Silicon heterojunction solar cells with electron selective TiO<sub>x</sub> contact. *Sol Energy Mater Sol Cells*. 2016;150:32-38. doi:10.1016/j.solmat.2016.01.020
85. Yoshikawa, K., Kawasaki, H., Yoshida, W., Irie, T., Konishi, K., Nakano, K., Uto, T., Adachi, D., Kanematsu, M., Uzu, H. and Yamamoto, K., 2017. Silicon heterojunction solar cell with interdigitated back contacts for a photoconversion efficiency over 26%. *Nature energy*, 2(5), pp.1-8.
86. Yu, C., Xu, S., Yao, J. and Han, S., 2018. Recent advances in and new perspectives on crystalline silicon solar cells with carrier-selective passivation contacts. *Crystals*, 8(11), p.430. doi:10.3390/cryst8110430
87. Zeng, Y., Peng, C.W., Hong, W., Wang, S., Yu, C., Zou, S. and Su, X., 2022. Review on metallization approaches for high-efficiency silicon heterojunction solar cells. *Transactions of Tianjin University*, 28(5), pp.358-373. *Transactions of Tianjin University* (2022) 28:358–373 <https://doi.org/10.1007/s12209-022-00336-9>.
88. Zhao, Y., Procel, P., Han, C., Cao, L., Yang, G., Özkol, E., Alcañiz, A., Kovačević, K., Limodio, G., Santbergen, R. and Smets, A., 2023. Strategies for realizing high-efficiency silicon heterojunction solar cells. *Solar Energy Materials and Solar Cells*, 258, p.112413. DOI 10.1016/j.solmat.2023.112413